

Cheilostome Bryozoa from the Upper Cretaceous Himenoura Group, Kyushu, Japan

Authors: Dick, Matthew H., Sakamoto, Chika, and Komatsu, Toshifumi

Source: Paleontological Research, 22(3) : 239-264

Published By: The Palaeontological Society of Japan

URL: <https://doi.org/10.2517/2017PR022>

The BioOne Digital Library (<https://bioone.org/>) provides worldwide distribution for more than 580 journals and eBooks from BioOne's community of over 150 nonprofit societies, research institutions, and university presses in the biological, ecological, and environmental sciences. The BioOne Digital Library encompasses the flagship aggregation BioOne Complete (<https://bioone.org/subscribe>), the BioOne Complete Archive (<https://bioone.org/archive>), and the BioOne eBooks program offerings ESA eBook Collection (<https://bioone.org/esa-ebooks>) and CSIRO Publishing BioSelect Collection (<https://bioone.org/csiro-ebooks>).

Your use of this PDF, the BioOne Digital Library, and all posted and associated content indicates your acceptance of BioOne's Terms of Use, available at www.bioone.org/terms-of-use.

Usage of BioOne Digital Library content is strictly limited to personal, educational, and non-commercial use. Commercial inquiries or rights and permissions requests should be directed to the individual publisher as copyright holder.

BioOne is an innovative nonprofit that sees sustainable scholarly publishing as an inherently collaborative enterprise connecting authors, nonprofit publishers, academic institutions, research libraries, and research funders in the common goal of maximizing access to critical research.

Cheilostome Bryozoa from the Upper Cretaceous Himenoura Group, Kyushu, Japan

MATTHEW H. DICK¹, CHIKA SAKAMOTO² AND TOSHIFUMI KOMATSU³

¹Department of Biological Sciences, Faculty of Science, Hokkaido University, N10 W8, Sapporo, Hokkaido 060-0810, Japan (e-mail: mhdick@newmex.com)

²Graduate School of Science and Technology, Kumamoto University, 2-39-1 Kurokami, 2-chome, Kumamoto 860-8555, Japan

³Faculty of Advanced Science and Technology, Kumamoto University, 2-39-1 Kurokami, 2-chome, Kumamoto 860-8555, Japan

Received September 7, 2017; Revised manuscript accepted November 9, 2017

Abstract. Cheilostome bryozoans (Phylum Bryozoa; Order Cheilostomata) originated in the latest Jurassic but remained at low diversity until the late Albian–early Cenomanian, when they began an explosive radiation that has continued to the present day. Most knowledge of Late Cretaceous cheilostomes comes from Europe and the USA from deposits associated with the western Tethys Ocean. Only a few previous records of Cretaceous bryozoans exist from the margin of eastern Asia in the NW Pacific. We examined material from four localities of early–middle Campanian age in the Himenoura Group, Shimokoshikijima Island, Kagoshima Prefecture, southern Kyushu, Japan, and detected six cheilostome species but no cyclostomes. Two species were relatively common. For one of these, we erect the new genus *Kenocharixa* and describe a new species, *Kenocharixa kashimaensis*; we also transfer *Charixa goshouraensis* Dick, Komatsu, Takashima, and Ostrovsky and *Conopeum stamenocelloides* Gordon and Taylor to *Kenocharixa*. We describe the other common species as *Marginaria proluxa* sp. nov. We detected four species as a single specimen each and identified them only to genus (*Charixa* sp. A) or listed them as *Incertae sedis* (A, B and C). Among the six cheilostomes, five are primitive anascan-grade (malacostegan) species and one is an anascan-grade neocheilostome. Compared to Campanian–Maastrichtian bryozoan faunas in Europe and the USA, the Himenoura fauna is low in diversity and morphological disparity, with no cribrimorph or ascophoran species detected. Previous researchers have suggested that the NW Pacific biota became isolated from that of the Tethys in the latest Aptian–middle Albian interval. We advance the hypothesis that the Late Cretaceous bryozoan fauna in the NW Pacific is a low diversity relict of the fauna present when this isolation occurred. While Tethyan cheilostome lineages underwent a major radiation associated with the origins of cribrimorph and ascophoran frontal shields, the NE Pacific lineages failed to diversify at the same rate and remained at low diversity and disparity. Testing this hypothesis will require much further sampling in Cretaceous deposits along the margin of East Asia.

Key words: Bryozoa, cheilostome diversity, Cretaceous, isolation, morphological grade, Tethys

Introduction

Cheilostome bryozoans (Phylum Bryozoa, Class Gymnolaemata, Order Cheilostomata) originated in the latest Jurassic (Taylor, 1994) and existed at low diversity for about 60 my. Starting in the late Albian to early Cenomanian, they began an explosive radiation (Taylor, 1988a; Ostrovsky *et al.*, 2008) that has continued to the present. While cyclostome bryozoans dominated assemblages throughout the Early Cretaceous, a faunal turnover occurred in the Late Cretaceous so that cheilostomes became the dominant group. This turnover apparently occurred at different times in different areas; in Cenomanian to Turonian assemblages in northern Europe,

the ratio of cyclostome to cheilostome species was still roughly 3:1, whereas in a coeval assemblage in the Bagh Beds in India the ratio was reversed (Taylor and Badve, 1994).

Most knowledge of the Cretaceous radiation of cheilostomes comes from deposits in Europe and the USA associated with the western Tethys. Although Lower to Upper Cretaceous strata from brackish to marine habitats are widespread along the margin of eastern Asia (e.g. Komatsu and Maeda, 2005; Iba and Sano, 2007; Komatsu *et al.*, 2008), knowledge of Cretaceous cheilostomes from this region is extremely limited and is restricted to the Japanese archipelago. The only previous records are *Dysnoetocella? voighti* Nishizawa and Sakagami, 1997

of Campanian age from Shikoku Island; an unidentified malacostegan species of middle Cenomanian age from Hokkaido (Ostrovsky *et al.*, 2006); and an assemblage of six cheilostome species (three of which were described as *incertae sedis* due to limited, poorly preserved material) and one cyclostome from the upper Albian to lower Cenomanian Goshoura Group on Kyushu (Dick *et al.*, 2013).

Elucidating the diversity and composition of Late Cretaceous cheilostome assemblages along the continental margin of eastern Asia is of evolutionary and biogeographical interest (Dick *et al.*, 2013). While the carbonate platform biota in NE Asia (NW Pacific) belonged to the Tethyan biotic realm through most of the Early Cretaceous, Mesogean (Cretaceous Tethys) key and indicator taxa (rudists, dasycladacean algae, hermatypic corals, stromatoporoids, nerineacean gastropods, orbitolinid foraminifers, and calcareous red algae) and coated grains disappeared from carbonate platforms along the margin of NE Asia in two stages from late Aptian to middle Albian times (Iba and Sano, 2007, 2008). This demise of the Asian carbonate platform biota suggests that the Tethyan and NE Asian biotas became isolated from one another. Reflecting this isolation, many endemic species began to appear in molluscan genera in the NW Pacific in the middle Albian, signaling the beginning of an endemic North Pacific fauna. It is not clear how this late Aptian to middle Albian biotic turnover in the NW Pacific affected the composition and diversity of bryozoans, as no bryozoan assemblages of this age have yet been documented in the region.

The Upper Cretaceous Himenoura Group, consisting of non-marine and marine siliciclastics, crops out on the central west side of Kyushu, Japan (Ueda and Furukawa, 1960; Tashiro *et al.*, 1986; Komatsu *et al.*, 2008; Kojo *et al.*, 2011), and includes marine deposits of Santonian to Campanian age containing abundant molluscan fossils (Komatsu *et al.*, 2008). The upper part of the Himenoura Group is exposed in the Kashima area (Figure 1A), northern Shimokoshikijima Island (Kagoshima Prefecture), off the SW coast of Kyushu. These brackish to marine, lower to middle Campanian deposits contain abundant molluscan fossils (Tanaka and Teraoka, 1973; Tashiro, 1976; Inoue *et al.*, 1982; Kanoh *et al.*, 1989; Komatsu *et al.*, 2014), among which bryozoans are moderately common, often encrusting bivalves. The goal of this study was to document the composition of this Campanian bryozoan assemblage for comparison with coeval Tethyan bryozoan assemblages.

Material and methods

Geological setting and fossil sites

Units U-I, U-IIa–d, and U-IIIa–d of the Himenoura

Group are exposed on Shimokoshikijima Island (Tashiro, 1976; Kanoh *et al.*, 1989), with U-IIb–d and U-IIIa–b occurring in our study area (Figures 1, 2) in the Kashima region (Figure 1A, B). U-II is composed mainly of fossiliferous marine sandstone and mudstone intercalated with abundant shell concentrations that include the lower and middle Campanian inoceramids *Sphenoceras* *orientalis* and *S. schmidtii*, and the ammonoids *Eupachydiscus haradai* and *Eulophoceras* sp. (Noda *et al.*, 1995; Miyake *et al.*, 2011; Komatsu *et al.*, 2014; Misaki *et al.*, 2016). U-III consists of non-marine and shallow marine conglomerate, sandstone, and mudstone, and contains *Crassostrea* oyster banks, trioniid bivalves, and isolated dinosaur remains (Toshimitsu *et al.*, 1990; Miyake *et al.*, 2011; Komatsu *et al.*, 2014). Aramaki *et al.* (2013) reported middle Campanian radiolarian assemblages characterized by *Amphipyndax pseudoconulus* from the upper part of U-III.

Bryozoans were collected at four localities (Figure 1): Loc. 1 (Figure 2A), NE side of Tsuburazaki Point (31°47'10"N, 129°47'24"E); Loc. 2 (Figure 2E, F), Kumagasehana Point (31°45'37"N, 129°48'13"E); Loc. 3 (Figure 2B–D), Ukimizuura (31°45'18"N, 129°47'09"E); and Loc. 4, Higireura (31°44'25"N, 129°46'48"E). Bryozoans occur commonly in unit U-IIb at Locs. 1 and 3, and uncommonly in unit U-IIb at Loc. 4 and in unit U-IIIa at Loc. 2 (Figures 3–6). Unit IIb is dominated by dark gray mudstone containing very fine, parallel-laminated sandstones that accumulated in an outer shelf environment. U-III is characterized by sandstones containing *Crassostrea* oyster banks and tidal bundles (Dalrymple, 1992) that were deposited in intertidal to subtidal environments.

At Locs. 1, 3, and 4, outer shelf mudstones contain abundant lenticular shell concentrations 1–5 cm thick consisting of fragments of inoceramid shells (which are commonly encrusted by bryozoans) (Figure 2C, D), serpulid tubes, and corals. Fragments of branched, erect bryozoan colonies also occasionally occur in these shell concentrations. At Loc. 2, the *Crassostrea* oyster banks are overlain by a concentration of mainly broken *Crassostrea* shells that also occasionally contain bryozoans.

Collection and handling of specimens

Bryozoans were collected by breaking apart fossiliferous rocks with hammer and chisel and searching by eye and with a hand lens for bryozoan colonies encrusting the surfaces of fossil bivalves and the molds left by bivalves in the rock matrix, and for fragments of erect colonies in the matrix itself. Cretaceous bryozoans in Japan are usually detected as the basal surface of the colony visible on the surface of a rock cast or mold left by the original, usually molluscan substrate, the colony having sepa-

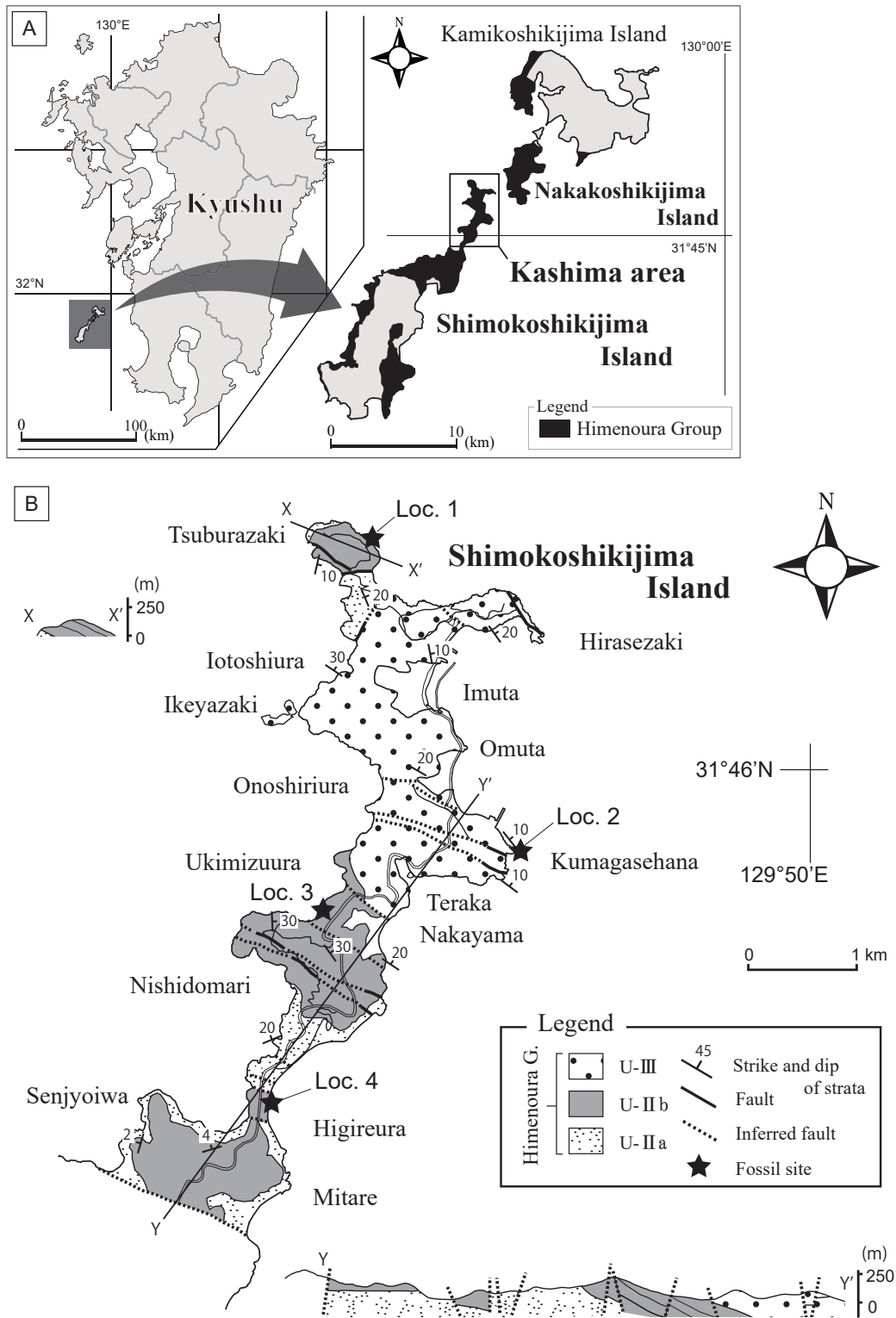


Figure 1. A, map of Kyushu, southern Japan (left), showing the location of the Koshikijima Islands (shaded box), enlarged on the right. Unshaded box on right indicates the area enlarged in panel B. B, geological map of the northern part of Shimokoshikijima Island, indicating strata of the Himenoura Group. Lines X–X' and Y–Y' indicate the positions of the cross-sections at the upper left and lower right, respectively.

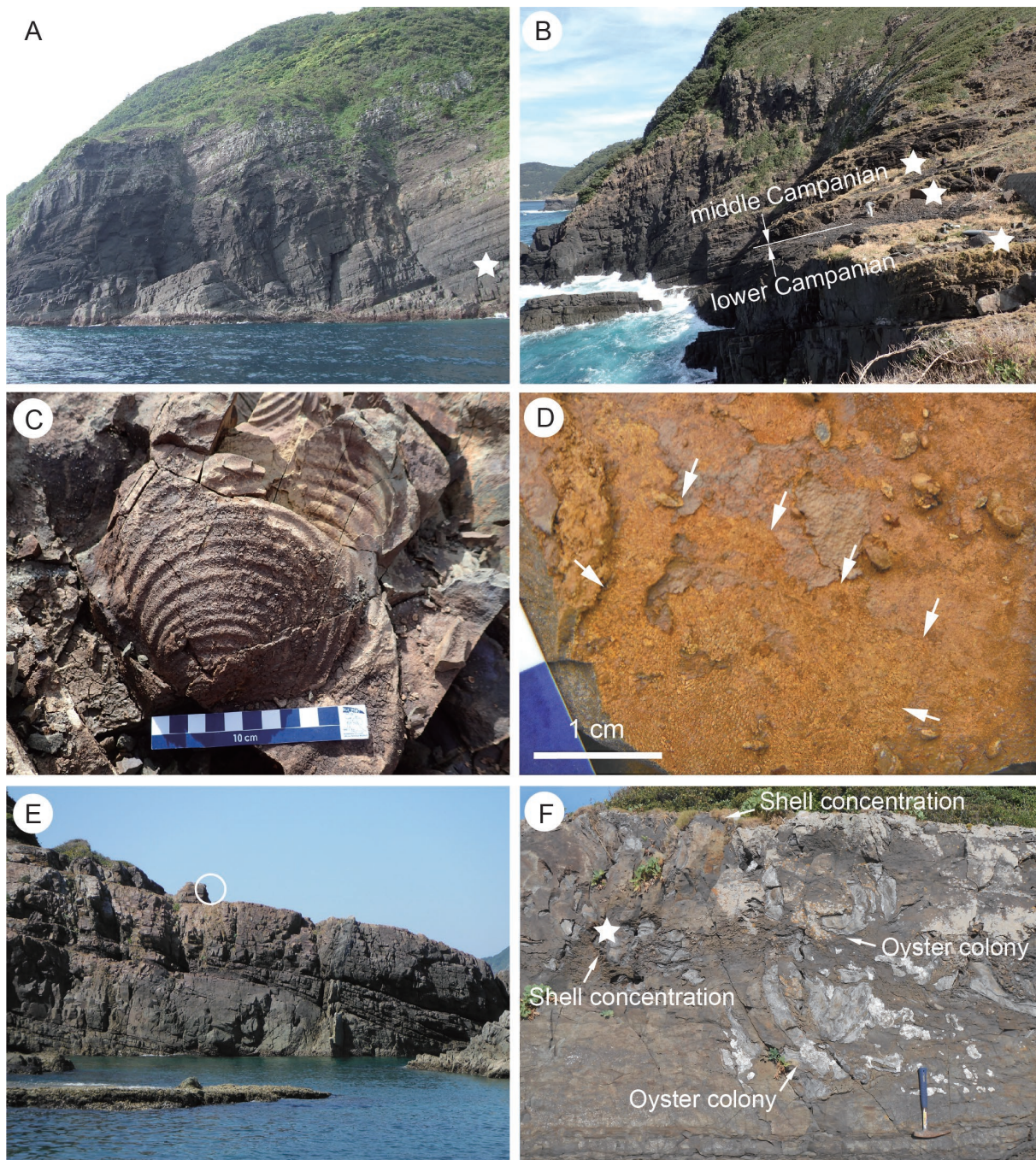


Figure 2. Selected photographs from collecting localities on Shimokoshikijima Island. **A**, locality 1, Tsuburazaki. Star indicates where bryozoans were found. **B**, locality 3, Nakayama (western area). Stars indicate bryozoan sites. **C**, locality 3, *Inoceramus cycloides* encrusted by bryozoan colonies. **D**, locality 3, outer mold of large inoceramid shell fragment. Arrows indicate the outline of a large bryozoan colony. **E**, locality 2, Ukimizuura. Circle indicates the site where a specimen of *Incertae sedis C* was collected. **F**, enlargement of the rock face circled in panel E, showing the positions of bivalve shell concentrations and oyster colonies. Star indicates where *Incertae sedis C* was collected.

rated from the shell. In many cases, natural dissolution of the skeleton of the bryozoan colony itself leaves a mold from which a detailed vinyl polysiloxane (VPS) silicone

cast can be made, which can then be viewed by scanning electron microscope (SEM) (Dick *et al.*, 2009, 2013). The methods used in this study to prepare specimens,

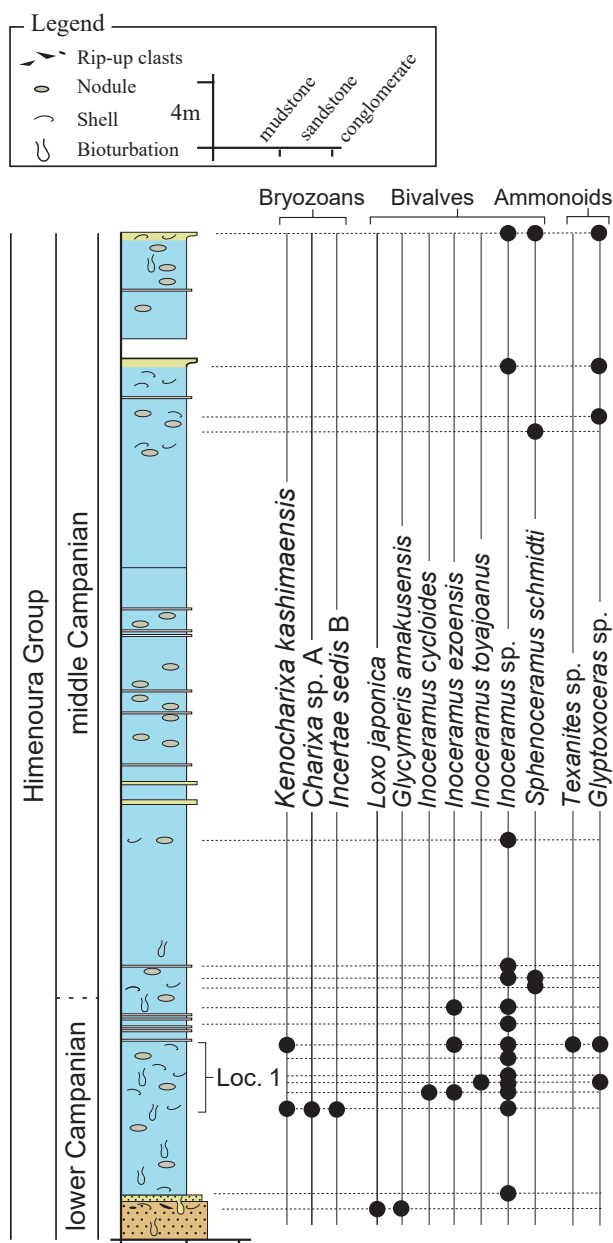


Figure 3. Stratigraphic column at Locality 1 (see Figure 1) within the Himenoura Group. Filled circles indicate the occurrences of bryozoan species, as well as of indicator bivalve and ammonoid species.

make VPS casts, and prepare the casts for SEM were as described by Dick *et al.* (2009). Bryozoan specimens and silicone casts were coated with Au in a JEOL JFC-1500 quick auto coater (JEOL Ltd., Tokyo) and images were captured with a JEOL JSM-6360LV scanning electron microscope (JEOL Ltd., Tokyo).

Zooidal characters were measured from SEM images by using ImageJ software (<http://rsbweb.nih.gov/ij/>); the

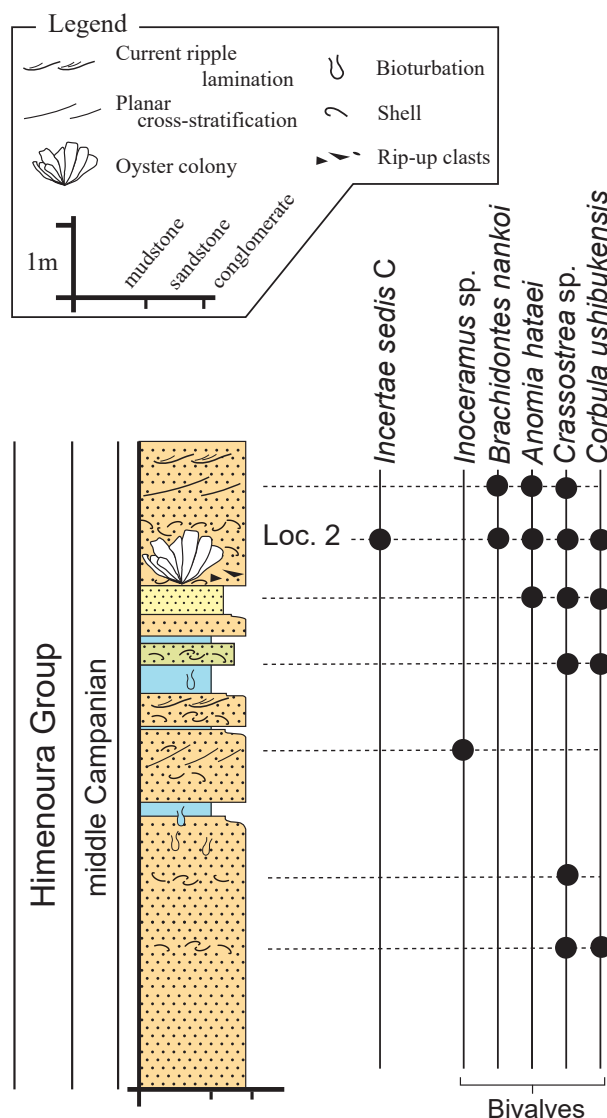


Figure 4. Stratigraphic column at Locality 2 (see Figure 1) within the Himenoura Group. Filled circles indicate the occurrence of the bryozoan *Incertae sedis C*, as well as of indicator bivalve species.

target sample size for measurements was 15 zooids in the zone of astogenetic repetition in each colony, although in some cases fewer adequate zooids were available. Specimen HimeL2-1 was photographed with a Nikon D5200 digital camera mounted on a Nikon SMZ1500 stereoscopic microscope, and zooidal measurements were made from photomicrographs after scales were determined with an ocular micrometer and a 1.00 mm objective rule divided into 0.01 mm units. Measurements of zooidal characters are defined in the text by combinations of the following abbreviations: Av, avicularium; Cp, zooid with

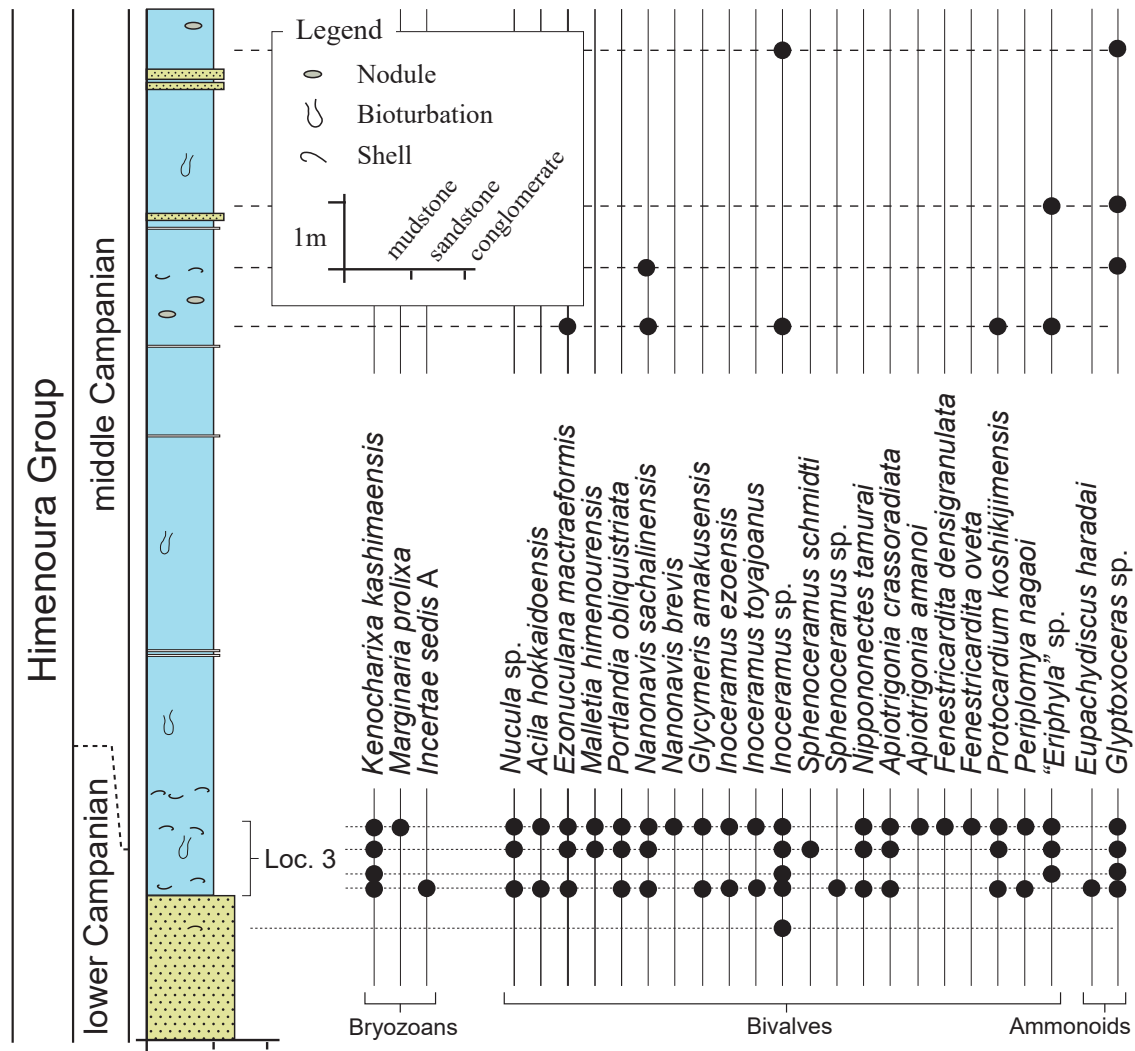


Figure 5. Stratigraphic column at Locality 3 (see Figure 1) within the Himenoura Group. Filled circles indicate the occurrences of bryozoan species, as well as of indicator bivalve and ammonoid species.

closure plate; Ip, interzooidal polymorph; Iz, interzooidal; L, length; Op, opesia; Ov, ovicell; W, width; Z, autozooid. For example, *ZOpL* = auto zooidal opesia length, *CpL* = length of zooid with closure plate, *IzAvL* = interzooidal avicularium length, and so forth.

All specimens, including type material and casts, have been deposited in the National Museum of Nature and Science (Department of Geology and Paleontology), Tsukuba, Japan, under catalog numbers with the prefix NMNS PA, with the number referring to both the specimen and the cast. Specimens examined in this study are listed in Table 1, with entries including both the NMNS PA number and the original specimen number; the table also indicates type specimens. The classification presented herein above the genus level is that of Gordon

(2017).

Systematic descriptions

Class Gymnolaemata Allman, 1856
 Order Cheilostomata Busk, 1852a
 Suborder Malacostegina Levinsen, 1902
 Superfamily Membraniporoidea Busk, 1852b
 Family Electridae Stach, 1937
 Genus *Kenocharixa* gen. nov.

Type species.—*Kenocharixa kashimaensis* sp. nov., by original designation.

Additional species.—We here transfer to *Kenocharixa* the species *Charixa goshouraensis* Dick, Komatsu,

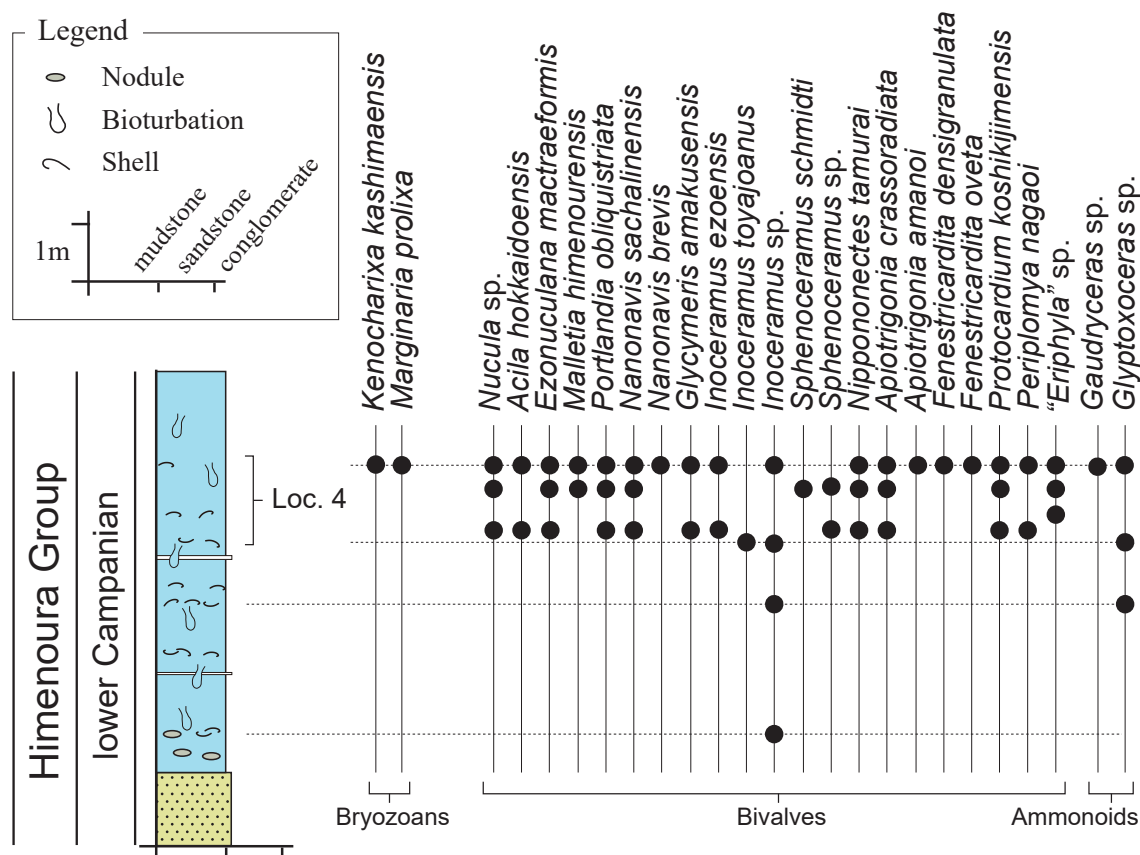


Figure 6. Stratigraphic column at Locality 4 (see Figure 1) within the Himenoura Group. Filled circles indicate the occurrences of bryozoan species, as well as of indicator bivalve and ammonoid species.

Takashima and Ostrovsky, 2013 and *Conopeum stamencelloides* Gordon and Taylor, 2015.

Etymology.—The name combines *Charixa*, referring to similarity to that genus, with “keno”, referring to the characteristic kenozooidal extensions filling interzooidal grooves.

Diagnosis.—Colony encrusting, unilaminar, sheet-like or erect, bilaminar. Gymnocyst moderate to negligible; long cauda lacking. Opesia occupying most of frontal surface, oval or elliptical in outline. Cryptocyst sloping, granulated. Zooids with closure plates scattered throughout colony, often grouped; variable in frequency. Spines lacking. Medium-sized kenozooids (here termed ‘interzooidal polymorphs’ to distinguish them from the smaller proximalateral kenozooids) present or absent; scattered throughout colony. Small kenozooids arise from proximalateral corners of zooids on one or both sides, sending out long extensions that fill interzooidal grooves. Zooids have distal and distolateral buttressed recesses leading to multiporous septula. Ancestrula initially buds three zooids, distally and distolaterally; ancestrula and several

generations of daughter zooids can have closure plates. Avicularia, ovicells lacking.

Remarks.—In the type species, most zooids bear paired, initially triangular kenozooids covering the proximal gymnocyst, a feature that along with the absence of avicularia and ovicells suggested placement in *Conopeum* Gray, 1848, the type species of which, *Millepora reticulum* Linnaeus, 1767, has similar kenozooids. Dick *et al.* (2013) discussed at length the taxonomic problems associated with *Conopeum*, noting that few Recent or fossil species currently placed in that genus show the same suite of characters as the type species. In particular, it is controversial whether paired proximalateral kenozooids are diagnostic for the genus. Dick *et al.* (2013) described from southern Japan another malacostegan species, *Charixa goshouraensis*, of late Albian–early Cenomanian age. The genus *Charixa* Lang, 1915 provided a reasonable but not entirely satisfactory fit for that species, which has a multiserial colony with contiguous zooids and commonly has zooids with closure plates. In *Charixa*, colonies tend to be pluriserial with irregularly arranged, partly contigu-

Table 1. List of specimens examined in this study. For all but two specimens, SEM images were made from silicone casts. *Incertae sedis* B was examined by SEM directly, without casting, and *Incertae sedis* C was examined by light microscopy.

NMNS PA-	Specimen number	Locality	Type	NMNS PA-	Specimen number	Locality	Type
<i>Kenocharixa kashimaensis</i> sp. nov.				<i>K. kashimaensis</i> sp. nov. (continued)			
18399	Hime1-18	3	Holotype	18427	Hime1-28	3	–
18400	Hime1-1	3	Paratype	18428	Hime4c-6	1	–
18401	Hime1-8	3	Paratype	18429	Hime4c-7	1	–
18402	Hime1-9	3	Paratype	18430	Hime4c-5	1	–
18403	Hime1-16	3	Paratype	18431	Hime4c-8	1	–
18404	Hime1-17	3	Paratype	18432	Hime4c-9	1	–
18405	Hime1c-3	3	Paratype	18433	Hime2c-3	4	–
18406	Hime1c-8	3	Paratype	<i>Charixa</i> sp. A (with <i>K. kashimaensis</i>)			
18407	Hime1c-9	3	Paratype	18434	Hime4c-5	1	–
18408	Hime1c-6a	3	Paratype	<i>Incertae sedis</i> A (with <i>K. kashimaensis</i>)			
18409	Hime4c-3	1	Paratype	18435	Hime1c-3	3	–
18410	Hime4c-4	1	Paratype	<i>Incertae sedis</i> B			
18411	Hime1-2	3	–	18436	Hime4-1	1	–
18412	Hime1-3	3	–	<i>Incertae sedis</i> C			
18413	Hime1-4	3	–	18437	HimeL2-1	2	–
18414	Hime1-5	3	–	<i>Marginaria prolixa</i> sp. nov.			
18415	Hime1-6	3	–	18438	Hime1-7	3	Holotype
18416	Hime1-12	3	–	18439	Hime1-15	3	Paratype
18417	Hime1-13	3	–	18440	Hime1-22	3	Paratype
18418	Hime1-14	3	–	18441	Hime1-23	3	Paratype
18419	Hime1-25	3	–	18442	Hime1-19	3	–
18420	Hime1c-1	3	–	18443	Hime1-20	3	–
18421	Hime1c-2	3	–	18444	Hime2c-2	4	–
18422	Hime1c-4	3	–				
18423	Hime1c-6c	3	–				
18424	Hime1c-7b	3	–				
18425	Hime1c-x	3	–				
18426	Hime1-26	3	–				

ous zooids, and closure plates are generally uncommon. With regard to generic placement, we realized that both *Charixa goshouraensis* and the new species from Shimo-

koshikijima resembled species in the Cretaceous genera *Charixa* and *Spinicharixa* Taylor, 1986a, but shared a unique character not present in the latter two genera—

proximolaterally derived kenozooids that ramify into the surrounding interzooidal grooves, eventually connecting with rami from other kenozooids and filling the grooves. We thus erect the new genus *Kenocharixa* for these two species from the Cretaceous of southern Japan.

We also transfer to *Kenocharixa* the species *Conopeum stamenocelloides* Gordon and Taylor, 2015, described from the Eocene of New Zealand; this species resembles *Kenocharixa kashimaensis* in having paired, triangular proximolateral kenozooids that extend into and fill the interzooidal grooves, and autozooids with closure plates. The cryptocyst in *C. stamenocelloides* is much wider than in *K. kashimaensis*, especially proximally, whereas that in *K. goshouraensis* is intermediate between the two, and generally wider proximally than laterally. *Kenocharixa goshouraensis* lacks the obligate paired, triangular kenozooids seen in the other two species, but they are often paired and triangular (e.g. Dick *et al.*, 2013: figs. 7B, D, E; 8B). *Conopeum stamenocelloides* differs from *K. kashimaensis* and *K. goshouraensis* in forming an erect, bilaminar colony and in having interzooidal connections in the form of small mural septula (Gordon and Taylor, 2015). The difference in colony form is not an impediment to placement in the same genus, as various cheilostome genera contain both encrusting unilaminar and erect species (e.g. *Thalamoporella*, *Porella*). The nature of the interzooidal connections need also not be an impediment; the septula in *C. stamenocelloides* appear to be set in mural depressions (Gordon and Taylor, 2015: fig. 21A, B) that may be the vestiges of the buttressed recesses seen in *K. kashimaensis* and *K. goshouraensis*.

Characters in *Kenocharixa* patchily overlap with those in *Spinicharixa* and *Charixa*. The primary difference between the latter two genera is that zooids in *Spinicharixa* have numerous spine bases around the margin of the cryptocyst, whereas those in *Charixa* lack spine bases or have only a small distal pair (Taylor, 1986a). The three species we place in *Kenocharixa* appear to lack spine bases altogether, a feature shared with some species in *Charixa* but distinguishing it from *Spinicharixa*. Taylor (1986a) also considered *Spinicharixa* and *Charixa* to differ in the degree of colony coherence, with species in *Spinicharixa* having pluriserial or multiserial colonies with regularly arranged zooids, and those in *Charixa* having pluriserial colonies with irregularly arranged zooids. This difference is not as clear as with the presence or absence of marginal spines; of the two species currently placed in *Spinicharixa*, *S. pittii* Taylor, 1986a has a multiserial colony with zooids in regular quincuncial arrangement, whereas *S. dimorpha* Taylor, 1986a has a pluriserial colony with zooids less tightly packed, as is more typical of *Charixa*. The three species we place in *Kenocharixa* have multiserial, sheet-like colonies with tightly packed

zooids, although the arrangement of zooids is less regular in *K. goshouraensis* than in the other two. The frequency of closure plates may also provide a useful diagnostic character; zooids with closure plates appear to be variably present and generally uncommon in species of *Spinicharixa* and *Charixa*, but more common in two of the species we place in *Kenocharixa*; Gordon and Taylor (2015) did not observe them in *K. stamenocelloides*, although they examined only two small specimens. Interestingly, the key character separating *Kenocharixa* from *Spinicharixa* and *Charixa*—the ramifying kenozooids—occurs in rudimentary form in *Charixa*; one of Taylor's (1986a: fig. 7c, p. 206) figures shows a kenozooid arising from the fusion of proximal buds from several autozooids and sending short extensions into interzooidal grooves.

Kenocharixa kashimaensis sp. nov.

Figures 7, 8

Diagnosis.—Colony encrusting, unilaminar, sheet-like. Zooids elongate-oval, gymnocyst negligible; ope-sia occupying most of frontal area; mural rim narrow, coarsely granulose. Spines, ovicells, and avicularia lacking. Paired triangular kenozooids at proximal corners of zooids. Zooids with closure plates uncommon, same size as autozooids, usually grouped. Small interzooidal polymorphs occur sparsely among autozooids. Zooids interconnect via buttressed recesses leading to multiporous septula. Ancestrula and periancestrular zooids produce closure plates.

Etymology.—The specific name is an adjective referring to Kashima, the municipality in which the type locality is located.

Material examined.—Thirty-seven specimens from Locs. 1, 3, and 4. Holotype, NMNS PA18399 (Loc. 3). Paratypes, NMNS PA18400–18410. See Table 1.

Measurements.—Measurements from autozooids and closure plate zooids are in Table 2. Interzooidal polymorphs: $IpL = 0.23\text{--}0.39$ mm (0.292 ± 0.048 mm); $IpW = 0.12\text{--}0.23$ mm (0.173 ± 0.030 mm); $IpOpL = 0.05\text{--}0.17$ mm (0.103 ± 0.028 mm); $IpOpW = 0.04\text{--}0.09$ mm (0.066 ± 0.013 mm) [$n = 15$ from five colonies]. Ancestrula, NMNS PA19409: $L = 0.241$ mm; $W = 0.150$ mm; $OpL = 0.086$ mm; $OpW = 0.076$ mm [$n = 1$].

Description.—Colony encrusting, unilaminar, sheet-like (Figure 7A). Zooids in large parts of colony arranged in long, unbranched columns offset from one another one-half zooid length, giving rise to quincuncial pattern (Figure 7A). Large sectors of colony contain strictly parallel columns with no bifurcations; new sectors arise by distal-distolateral bifurcations on zooids along one side of single column. Autozooids (Figure 7B) elongate oval, delineated by narrow groove; gymnocyst negligible, cov-

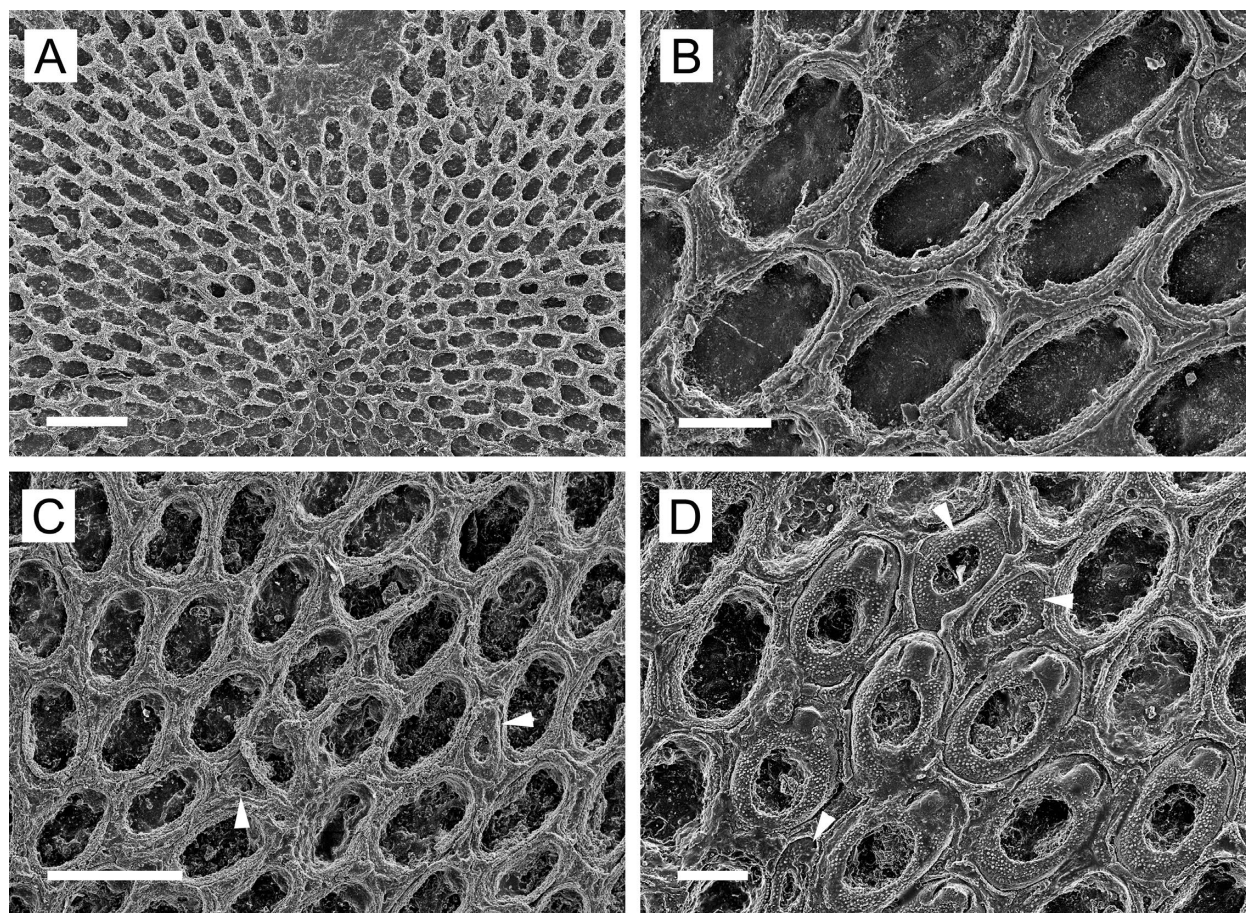


Figure 7. *Kenoscharixa kashimaensis* sp. nov., SEM images of silicone casts from colony molds. **A**, paratype NMNS PA18408, colony view showing colony-wide budding pattern; **B**, paratype NMNS PA18400, autozooids without heavy secondary calcification; **C**, paratype NMNS PA18405, autozooids and interzooidal polymorphs (arrowheads); **D**, holotype, NMNS PA18399, autozooids, zooids with closure plates, and large interzooidal polymorphs (arrowheads). Scale bars: 1.0 mm (A); 0.20 mm (B, D); 0.50 mm (C).

ered by kenozooids. Cryptocyst moderately wide proximally and laterally around opesia, sloping at steep angle (Figure 8B), coarsely granulose; opesia occupying most of frontal surface. Most zooids produce paired triangular kenozooids (Figures 7B; 8B, C) proximolaterally; kenozooidal surface coarsely granulose, cryptocystal; kenozooids sometimes merging, forming single, broad proximal kenozooid (Figure 7B). In some cases, central opening of kenozooid seen to lead to one or two pores in proximal gymnocyst of underlying autozooid. Kenozooids extend lobes of calcification into adjacent interzooidal grooves (Figure 7B, D); with age, lobes completely fill zooidal grooves (Figures 7C; 8A, B), eventually rising above level of mural rim (Figure 8C) and forming coarse, nodular thickening covering proximal end of zooids (Figure 8D, E). Interzooidal polymorphs occur uncommonly among autozooids; usually much smaller than autozooids (arrowheads, Figure 7C) but occasionally nearly as large

(upper two arrowheads, Figure 7D), with elliptical opesial opening and rounded mural rim; rim coarsely granulose in zone around opesia but smooth around margin. Zooids with closure plates occur uncommonly, singly or in groups of two to seven (Figure 7D); opesia reduced, oval or elliptical in outline, surrounded by tumid, rounded, coarsely granulose cryptocystal rim, with narrow zone of smooth gymnocyst around margin; opercular impression smooth, surrounded by horseshoe-shaped groove corresponding to opercular margin. Interzooidal polymorphs can occur among zooids with closure plates (Figure 7D). Zooids interconnect via distal and paired distolateral buttressed recesses, each leading to multiporous septulum (Figure 8A). Ancestrula (Figure 8F) budding triplet of zooids distally and distolaterally; ancestrula, triplet of zooids, and some but not all zooids in second and third generations from ancestrula forming closure plates; ancestrula and first two generations of daughter zooids with tapering

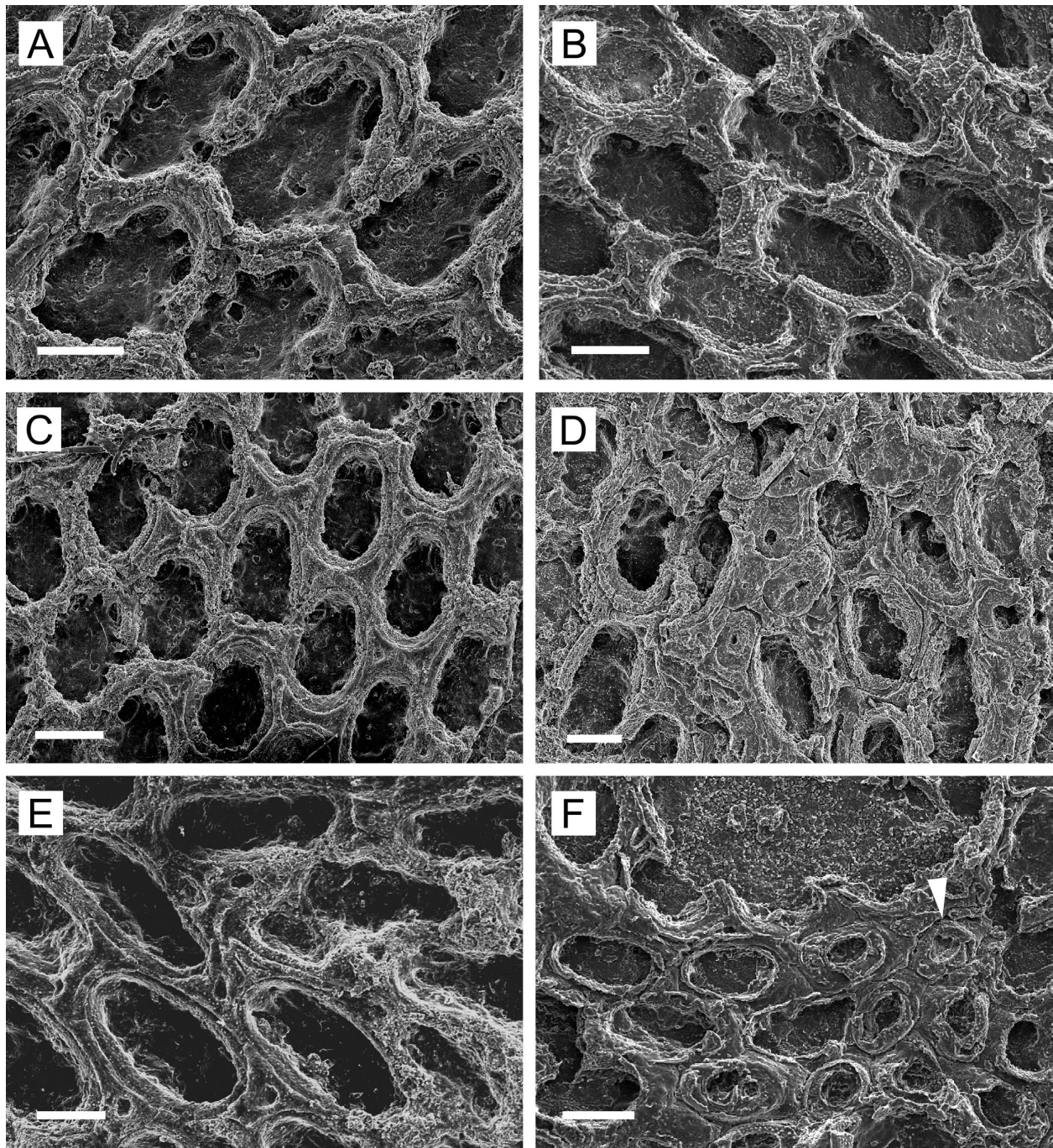


Figure 8. *Kenoscharixa kashimaensis* sp. nov., SEM images of silicone casts from colony molds. **A**, paratype NMNS PA18403, autozooids, showing interzooidal connections; **B**, paratype NMNS PA18409, heavily calcified autozooids, showing kenozooidal extensions in interzooidal grooves raised above the mural rims; **C**, paratype NMNS PA18403, moderately heavily calcified autozooids; note nodular accumulation covering proximal gymnocyst of right-center zooid; **D**, specimen NMNS PA18419, very heavily calcified colony, with autozooids and interzooidal polymorphs; **E**, paratype NMNS PA18403 showing apparent diagenetic loss of secondary calcification as seen in zooids at right, leaving primary layer as seen in zooids at left; **F**, paratype NMNS PA18409, ancestrula (arrowhead); ancestrula and some zooids within three generations of ancestrula appear to have closure plates. Scale bars: 0.20 mm.

Table 2. Measurements (in millimeters) for *Kenocharixa kashimaensis* sp. nov. For each set of values, the range is followed by the mean and standard deviation. Areas 1 and 2 in NMNS PA18404 were different parts of the same colony in the zone of astogenetic repetition; in the last column, sample sizes are indicated separately for autozooids (AZ) and zooids with closure plates (CP), with measurements of the latter presented as the average of two values.

	Holotype		Paratype		Paratype NMNS PA18404			
	NMNS PA18399		NMNS PA18405		Area 1		Area 2	
Autozooid length	0.44–0.51	0.477±0.020	0.45–0.60	0.501±0.042	0.38–0.49	0.431±0.026	0.52–0.64	0.560±0.041
Autozooid width	0.27–0.36	0.305±0.029	0.24–0.34	0.299±0.027	0.23–0.35	0.288±0.026	0.27–0.34	0.311±0.022
Autozooid opesia length	0.31–0.39	0.359±0.022	0.30–0.39	0.353±0.022	0.29–0.42	0.344±0.031	0.34–0.44	0.391±0.028
Autozooid opesia width	0.17–0.23	0.188±0.017	0.14–0.21	0.181±0.019	0.16–0.27	0.224±0.021	0.17–0.23	0.202±0.018
Closure plate zooid length	0.30–0.54	0.457±0.066	–	–	–	–	–	0.567
Closure plate zooid width	0.22–0.34	0.284±0.035	–	–	–	–	–	0.339
Closure plate opesia length	0.12–0.24	0.202±0.038	–	–	–	–	–	0.289
Closure plate opesia width	0.08–0.17	0.135±0.025	–	–	–	–	–	0.171
Sample size (<i>n</i>)	15		15		41		AZ = 15 CP = 2	

proximal gymnocyst lacking kenozooids, which appear in some zooids in third generation from ancestrula. Intramural budding not observed.

Remarks.—The species most similar to *Kenocharixa kashimaensis* is the congener *K. goshouraensis* (Dick *et al.*, 2013). Zooid size is similar, and in the zone of astogenetic repetition both species have elongate zooids with the opesia occupying most of the frontal area (compare Figure 7A herein with Dick *et al.*, 2013: fig. 8A). The arrangement of zooids in the colony is less regular in *K. goshouraensis*, where zooids in some parts of the colony occur in quincunx but in other parts are arranged in non-offset columns, so that zooids are side-by-side in rows. Zooids of *K. goshouraensis* generally have a more extensive gymnocyst, especially proximally but also laterally, resulting in larger interzooidal grooves; in the zone of astogenetic change, the proximal gymnocyst can be extensive, with the opesia oval and only half as long as the zooid. As in *K. kashimaensis*, the kenozooids in *K. goshouraensis* that later elongate in the interzooidal grooves originate proximolaterally, but they are initially smaller, less regularly triangular, and less stereotyped in position (they can be paired, or lacking on one or both sides), and they tend to elongate primarily in the lateral groove between zooidal columns, rather than also filling the transverse groove between zooids (Dick *et al.*, 2013: fig. 7A–E). *Kenocharixa goshouraensis* lacks the medium-sized interzooidal polymorphs seen in *K. kashimaensis*. The closure plates are similar between the two

species, but those in *K. kashimaensis* are frontally tumid and convex, whereas those in *K. goshouraensis* are somewhat sunken inside the raised margin and have a smaller opesia. In *K. goshouraensis*, some intramurally budded zooids were seen to form closure plates (Dick *et al.*, 2013: fig. 7F), whereas no intramural budding was observed in *K. kashimaensis*. The ancestrular budding pattern is identical in the two species; in both, the ancestrula gives rise to a triplet of daughter zooids distally and distolaterally, and the ancestrula and at least some zooids in the first three generations from the ancestrula have closure plates.

Zooids like those in Figure 7B might be interpreted as lacking heavy secondary calcification because they are young. However, Figure 8E shows less heavily calcified zooids adjacent and distal to heavily calcified zooids, suggesting that the former represent instead a basal primary layer of calcification that is typically overlain by a heavy secondary layer, with the latter having been diagenetically dissolved in part of the colony. The mechanism by which this could occur is not clear.

Genus *Charixa* Lang, 1915

Type species.—*Charixa vennensis* Lang, 1915.

Charixa sp. A

Figure 9

Material examined.—NMNS PA18434 (Loc. 1), one

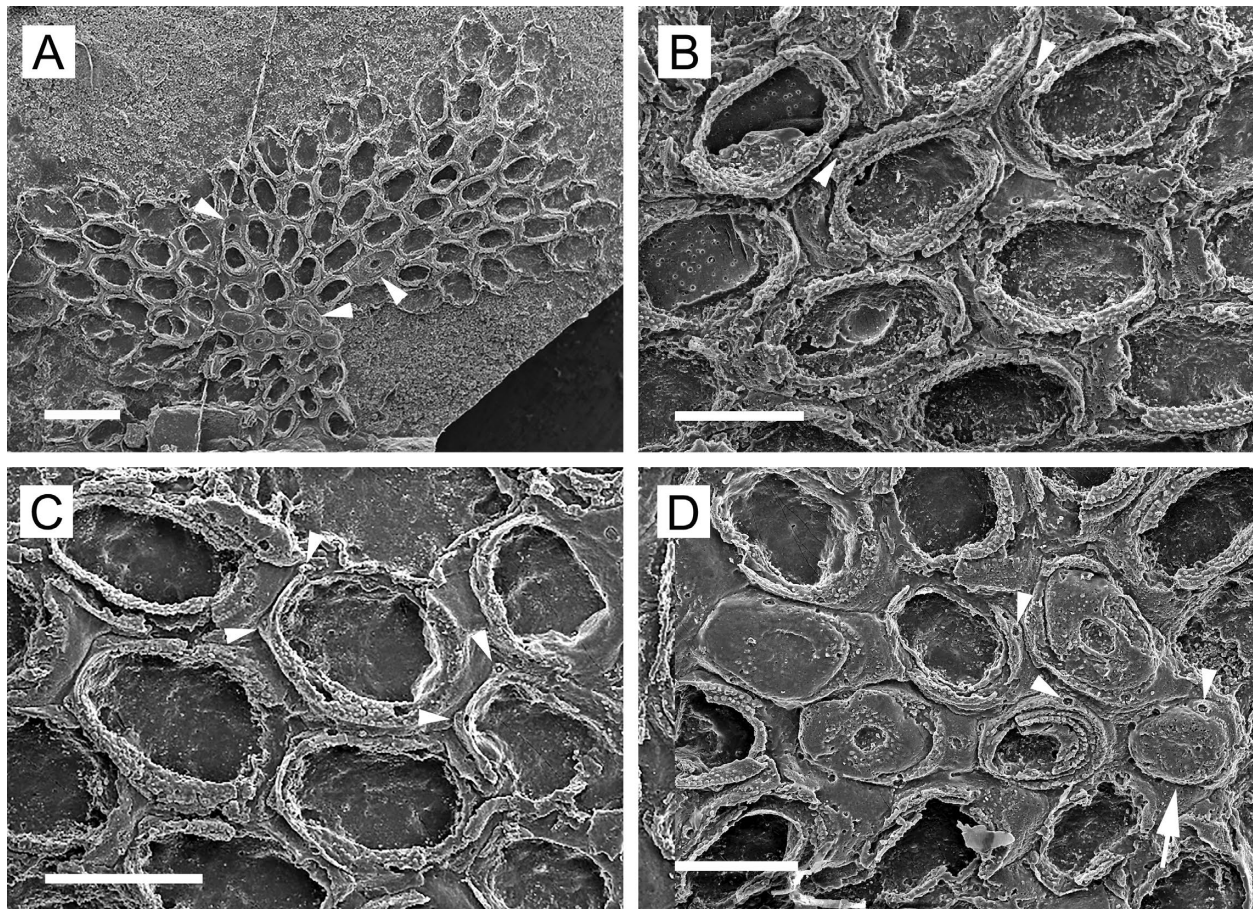


Figure 9. *Charixa* sp. A., specimen NMNS PA18434, SEM images of silicone cast from colony mold. **A**, view of colony. Arrowheads indicate interzooidal polymorphs (intramurally budded kenozooids). **B**, group of autozooids. Arrowheads indicate enlarged proximolateral spine bases. **C**, group of autozooids. Arrowheads indicate distal spine bases. **D**, ancestrula (arrow) and several generations of daughter zooids. Arrowheads indicate enlarged proximolateral spine bases. Scale bars: 0.5 mm (A); 0.20 mm (B, D); 0.25 mm (C).

small colony.

Measurements.— $ZL = 0.28\text{--}0.42$ mm (0.349 ± 0.037 mm); $ZW = 0.18\text{--}0.27$ mm (0.225 ± 0.026 mm); $ZOpL = 0.22\text{--}0.29$ mm (0.247 ± 0.024 mm); $ZOpW = 0.11\text{--}0.18$ mm (0.139 ± 0.021 mm); $n = 15$.

Description.—Colony (Figure 9A) encrusting, unilaminar, irregular, forming pluriserial lobes. Autozooids mostly arranged in quincunx; irregularly hexagonal or oval, delineated by deep, moderately wide groove. Gymnocyte (Figure 9C) evident proximally and proximolaterally, but probably not laterally in zone of astogenetic repetition; long proximal cauda lacking. Mural rim raised; granulated cryptocyst sloping, widest proximally, tapering in width laterally around opesia, lacking distally. Opesia (Figure 9A–C) occupying most of frontal area, elongate-oval or elliptical, widest in center or proximal half. Zooids bear pair of small spine bases at distolateral corners (arrowheads, Figure 9C); ancestrula, periances-

trular zooids (arrowheads, Figure 9D), and at least some autozooids (arrowheads, Figure 9B) show a larger spine base on one side in proximolateral part of mural rim. Interzooidal polymorphs occur as intramurally budded kenozooids (arrowheads, Figure 9A); center of frontal wall with small, elliptical or circular opesia. Ancestrula (arrow, Figure 9D) tatiform, with three pairs of spine bases; initially producing distal and paired distolateral daughter zooids; ancestrula possibly with closure plate, with traces of grooves corresponding to lateral opercular margins, although these apparent grooves could be casting artifacts, in which case the opesia is occupied by an intramurally budded kenozooid. Zooid distal to ancestrula with two intramural buds, with intramurally budded kenozooid forming inside those. Other zooids up to third generation from ancestrula with intramurally budded kenozooids. Proximolateral spine base enlarged on one side in ancestrula and two subsequent zooids (arrow-

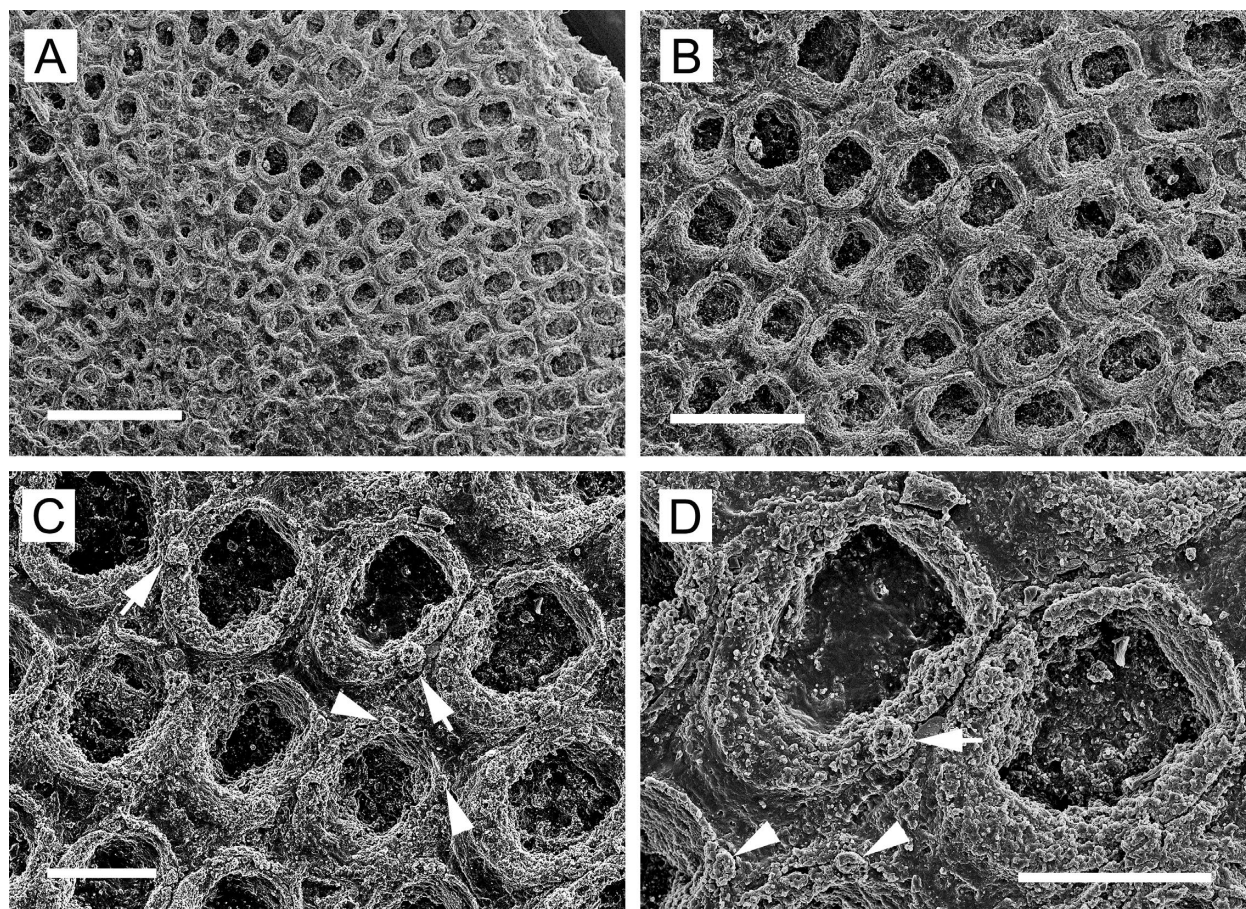


Figure 10. *Incertain sedis* A, specimen NMNS PA18435, SEM images of silicone cast from colony mold. **A**, view of colony; **B**, enlargement from panel A, showing autozooids; **C**, enlargement from panel B, showing autozooids with distal spine bases (arrowheads) and enlarged proximolateral structure of unknown function (arrows); **D**, enlargement of autozooids from panel C, showing spine bases (arrowheads) and proximolateral structure (arrow). Scale bars: 1.0 mm (A); 0.50 mm (B); 0.20 mm (C, D).

heads, Figure 9D). Ovicells and avicularia not observed. Interzooidal connections evident as distal and one or two pairs of distolateral buttressed recesses.

Remarks.—We assign this species to *Charixa* on the basis of the generic diagnosis by Taylor (1986a). The colony is irregularly arranged; zooids have a moderately well developed proximal gymnocyst; the cryptocyst is narrow and coarsely granulose; and in most zooids, spine bases appear to be limited to a small distal pair. The occurrence of a single larger, spine base proximolaterally on the mural rim in some zooids might represent an enlarged spine or scutum. *Incertain sedis* A (next description) shows a raised structure in the same position, which might suggest that the two species are related, perhaps comprising a previously unrecognized genus.

Incertain sedis A

Figure 10

Material examined.—NMNS PA18435 (Loc. 3), one colony, partly overgrown by *Kenocharixa kashimaensis*.

Measurements.— $ZL = 0.39\text{--}0.49$ mm (0.425 ± 0.032 mm); $ZW = 0.25\text{--}0.32$ mm (0.275 ± 0.021 mm); $OpL = 0.21\text{--}0.28$ mm (0.242 ± 0.021 mm); $OpW = 0.15\text{--}0.18$ mm (0.161 ± 0.010 mm); all measurements, $n = 15$.

Description.—Colony (Figure 10A) unilaminar, encrusting, sheet-like. Autozooids (Figure 10B, C) oval in outline, delineated by deep groove; arranged in irregular rows, with zooids only occasionally in quincuncial pattern (Figure 10A, B). Gymnocyst evident proximally and proximolaterally. Mural rim raised, rounded, widest proximally, tapering laterally, narrow distally, covered with cryptocystal granulation; cryptocyst steep, lacking distally. Opesia oval to elongate-oval; distal end straight. Some autozooids show coarse pair of short, erect spine

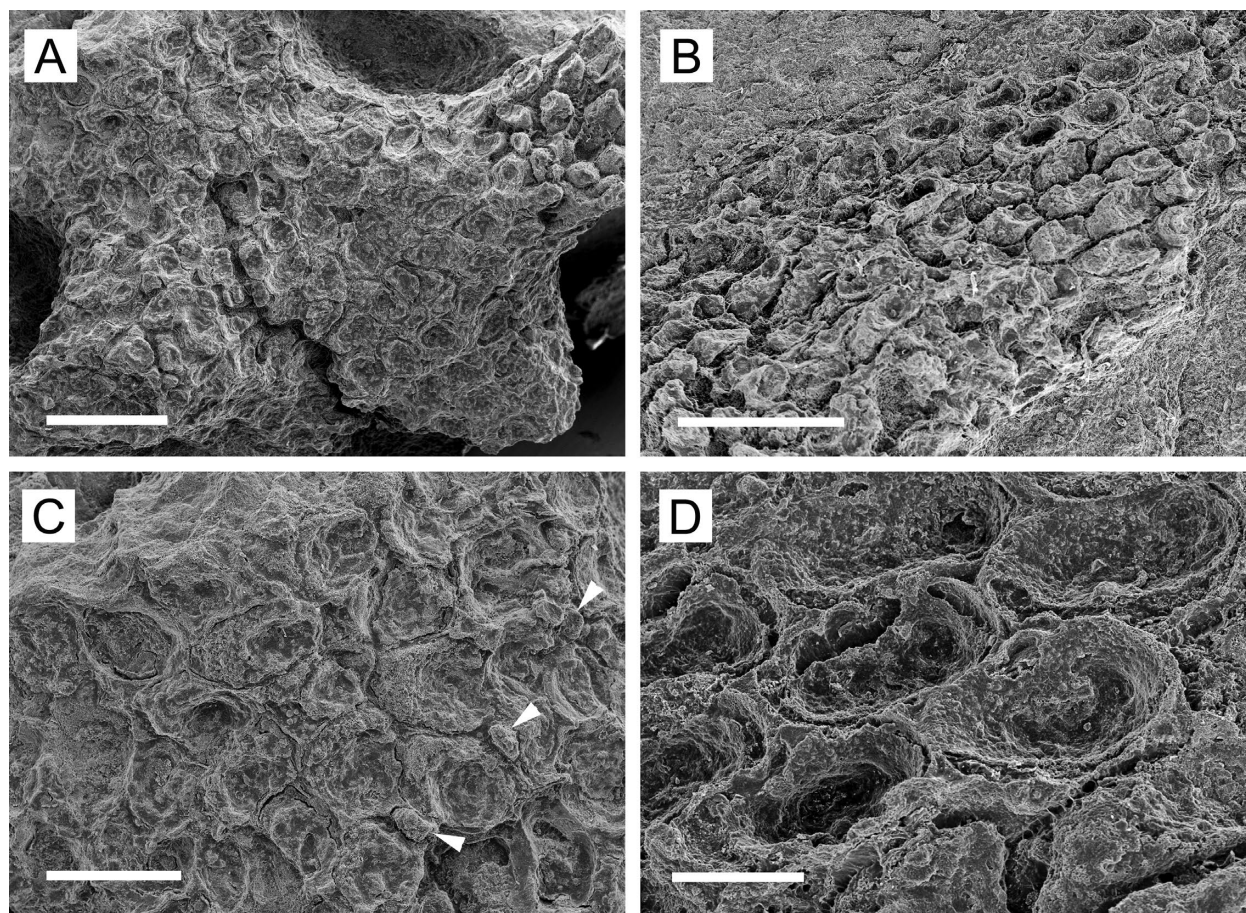


Figure 11. *Incertae sedis* B., specimen NMNS PA18436, SEM images of coated specimen. **A**, view of portion of erect colony: note bent, tubular zooids exposed at upper right; **B**, portion of colony surface with zooidal walls dissolved from around some zooids; **C**, view of colony surface showing small kenozooids (arrowheads) interspersed with autozooids; **D**, enlargement of autozooids, showing sloping, granulated cryptocyst. Scale bars: 1.0 mm (A, B); 0.50 mm (C); 0.20 mm (D).

bases at distolateral corners (arrowheads, Figure 10C, D); small spine bases possibly present around mural rim but difficult to discern. Most zooids have a raised nodule (arrows, Figure 10C) proximolaterally on mural rim on one or occasionally both sides; nodule of ambiguous structure but in some cases appearing hollow, with opening directed proximomedially (arrow, Figure 10D), possibly representing either small avicularium or base of large spine or scutum. No ovicells, avicularia, or closure plates observed; ancestrula not observed. Nature of interzooidal connections unclear.

Remarks.—This species, with zooids having a proximal gymnocyst and a pair of distolateral spines, might be placed in *Charixa*, although the extensive, coherent, sheet-like colony is unusual for that genus. The proximolateral nodular structure in *Incertae sedis* A is in the same position as the large proximolateral spine base in *Charixa* sp. A (above), raising the possibility that the two species

are closely related and represent an undescribed genus. The arrangement of zooids is different between the two; in *Charixa* sp. A, a mostly quincuncial arrangement of zooids appears early on (Figure 9A). While the ancestrula is not evident in our specimen of *Incertae sedis* A, the portion of the colony in the lower left of Figure 10A appears to be within the zone of astogenetic change, and there the zooids are arranged more in transverse rows than in quincuncial pattern. Clarifying the identity of *Incertae sedis* A will require additional, better material than the single specimen we have.

? Family Chiplonkarinidae Taylor and Gordon, 2007

Incertae sedis B

Figure 11

Material examined.—NMNS PA18436 (Loc. 1). The

specimen consists of two fragments of the same colony in rock matrix. One fragment is part of a frontally abraded branch, with the walls partly dissolved; the other comprises the terminal part of a multiramous branch, the original frontal surface mostly intact but with the walls dissolved in one of the branch ends, showing the internal orientation of the zooids. SEM images were taken from the intact specimen rather than from a cast.

Measurements.—Frontal $ZL = 0.28\text{--}0.37$ mm (0.313 ± 0.035 mm); Frontal $ZW = 0.22\text{--}0.36$ mm (0.269 ± 0.050 mm); $OpL = 0.12\text{--}0.17$ mm (0.141 ± 0.020 mm); $OpW = 0.11\text{--}0.18$ mm (0.125 ± 0.026 mm); $n = 6$.

Description.—Colony erect, with subcylindrical, cylindrical, or compressed branches; terminal fragment of one branch (Figure 11A) 7 mm long, 2.7 mm across, and 2 mm thick, with three rami at end; zooids completely surrounding branch. Zooids appear to be long, originating from central axis, overlapping one another for most of their length within branch, turning frontally near end (Figure 11A, upper right), with only most distal part of zooid showing frontally. Frontally exposed area irregular in outline: circular, oval, elliptical, or hexagonal. Opesia small; circular, oval, or elliptical; surrounded by sloping, granulated cryptocyst (Figure 11D). Gymnocyst lacking. Zooids interspersed with infrequent, irregularly occurring kenozooids (arrowheads, Figure 11C). No spine bases or oecia observed. Neither early astogeny nor basal portions of colony observed.

Remarks.—*Incertae sedis* sp. A resembles species in the Cretaceous family Chiplonkarinidae Taylor and Gordon, 2007. Chiplonkarinidae includes malacostegangrade cheilostomes in which the colony is primarily erect, with long, tubular zooids forming an inner endozone and an outer exozone. Hollow spines and closure plates are lacking; the gymnocyst is reduced or lacking; and the cryptocyst is narrow and does not form a proximal shelf (Taylor and Gordon, 2007). The details of the inner and outer zones differ among the four genera (Bock, 2017) presently placed in the family. In *Chiplonkarina* Taylor and Badve, 1995, autozooids are oriented parallel to the long axis of the branch in the endozone, but turn 90° into the exozone, where they become perpendicular to the branch surface. In *Heteroconopeum* Voigt, 1983, the proximal parts of autozooids in the endozone are polygonal in cross section, stacked vertically along the center of the branch to form prismatic cylinders, and have pores in both the lateral and transverse walls between zooids; zooids bend sharply into the exozone and open on the colony surface. The endozone occupies a much larger proportion of the cross-sectional area of a colony branch in *Heteroconopeum* than in *Chiplonkarina*. In *Zimmerella* Taylor, 2008, the colony is erect and dendroid, and branches have a scalloped axial lumen surrounded by

endozonal zooids, which are large and flask-shaped and produce exozonal zooids by frontal budding. Finally, in *Basslerinella* Taylor and McKinney, 2006, the colony forms bifoliate fronds rather than cylindrical branches; frontally, kenozooidal outgrowth fills in the spaces between autozooids and leaves a digitate edge surrounding the autozooidal opesia, which is extensive.

The autozooids in our specimen are clearly long, tubular, and turn frontally near their distal end (Figure 11A, upper right), suggesting the presence of an endozone and exozone, and indicating placement in Chiplonkarinidae. However, the frontal aspects of zooids evident in our specimen are not clearly identifiable with any of the four genera in this family. Determination of generic identity will ultimately require a cross-sectional view of a branch, and we were unwilling to risk damaging our only specimen, which in other respects is exceptionally good, to try to obtain this view. Further identification will require additional material.

Incertae sedis C

Figures 12, 13

Material examined.—NMNS PA18437 (Loc. 2). The specimen, consisting of calcified walls embedded in rock matrix, was observed and photographed through a stereomicroscope; no cast was possible. In life, one or more fully developed bryozoan colonies, and at least two young colonies, inhabited the highly concave interiors of two small *Crassostrea* valves that were probably fused together side by side when alive and remained fused either *in situ* or among shell rubble after death. In our specimen, the bryozoans occupy the outer surfaces of the interior casts left by the *Crassostrea* valves, with the mollusk shells having disappeared to expose the basal surfaces of the bryozoans. While many of the zooids in the light photomicrographs in Figures 12 and 13 appear to have the frontal walls exposed, these are actually the basal walls, and what appears to be the orifice (e.g. Figures 12D, E; 13D) in many zooids is actually a circular or oval, non-calcified distal portion of the basal wall. This is clearly evidenced by parts of colonies where the rock matrix has been partly or completely lost from the interiors of zooids, as is evident in Figure 13A; in a few of these zooids, the outline of the opesia (arrowheads, Figure 13A) and the shape of the interior of the zooidal frontal wall can be discerned. Of necessity, the description below is based mostly on the basal surface.

Measurements.—Primary axial zooids: $ZL = 0.65\text{--}0.82$ mm (0.738 ± 0.057 mm); $ZW = 0.10\text{--}0.19$ mm (0.152 ± 0.022 mm); $n = 13$. Secondary axial zooids: $ZL = 0.41\text{--}0.76$ mm (0.529 ± 0.105 mm); $ZW = 0.15\text{--}0.21$ mm (0.183 ± 0.018 mm); $n = 12$. Tertiary zooids:

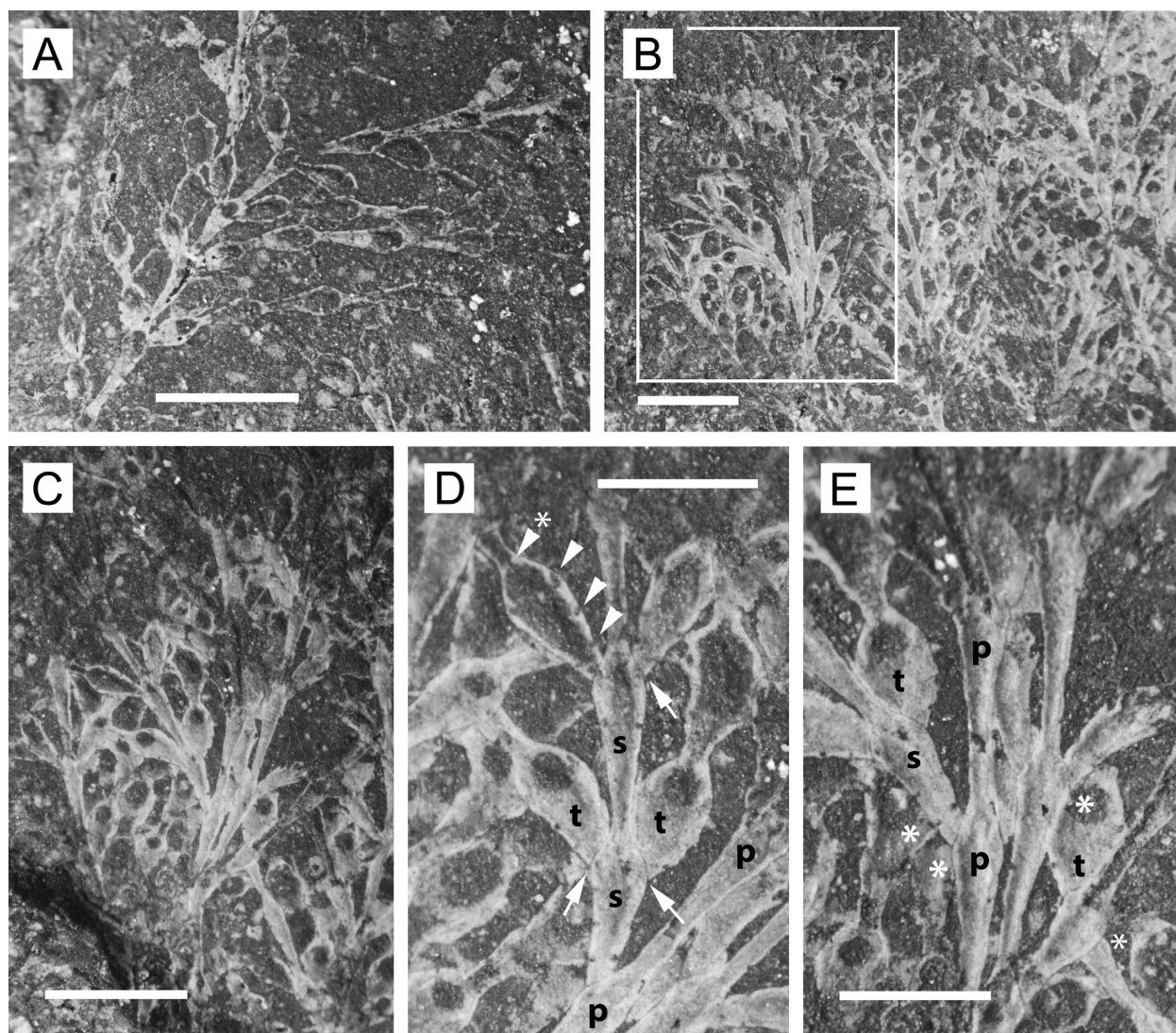


Figure 12. *Incertae sedis* C, light photomicrographs of intact specimen NMNS PA18437. **A**, young colony in basal view, showing primary and secondary axes, but few tertiary branches. **B**, branches from one or more older colonies, in basal view, showing jumbled arrangement of zooids. Box indicates approximate region enlarged in panel C. **C**, portion of colony in basal view, showing bipinnate branching pattern. **D**, enlargement from panel C; p, zooids in primary axis; s, zooids in secondary axis; t, tertiary zooids; arrowheads, tubular pore chambers in lateral wall; asterisked arrowhead, distal pore; arrows, fine sutures between mother and daughter zooids. **E**, enlargement from panel C; p, s, t as in panel D; asterisks, zooids (seen in basal view) overgrowing parts of other zooids. Scale bars: 1.0 mm (A–C); 0.50 mm (D, E).

ZL = 0.33–0.50 mm (0.411 ± 0.062 mm); ZW = 0.017–0.028 mm (0.237 ± 0.028 mm); $n = 11$. Orifice, secondary axial zooids: $OpL = 0.14$ mm; $OpW = 0.10$ – 0.11 mm; $n = 2$.

Description.—Colony encrusting; zooids in uniserial columns arranged in bipinnate branching pattern (Figures 12, 13), although capacity to become pluriserial exists (Figure 13D). Young colonies (Figures 12A, 13D) with branches well separated and distinct; older, larger colonies with branches irregularly and closely spaced, jumbled (Figure 12B). Zooids in primary axis of branch

(Figures 12D, E; 13B, C) each giving rise distally to next axial zooid in series and distolaterally to zooid on each side, initiating paired, opposite secondary axial branches. Zooids in secondary axis show same budding pattern, producing next axial zooid distally and pair of tertiary zooids distolaterally. Tertiary zooids typically bud subsequent tertiary zooids only distally, without giving rise to distolateral daughter zooids. Zooids in primary axis long and narrow, with long cauda (Figures 12E; 13B, C); non-calcified portion of basal wall typically lacking. Zooids in secondary axis wider and shorter on average (Figures

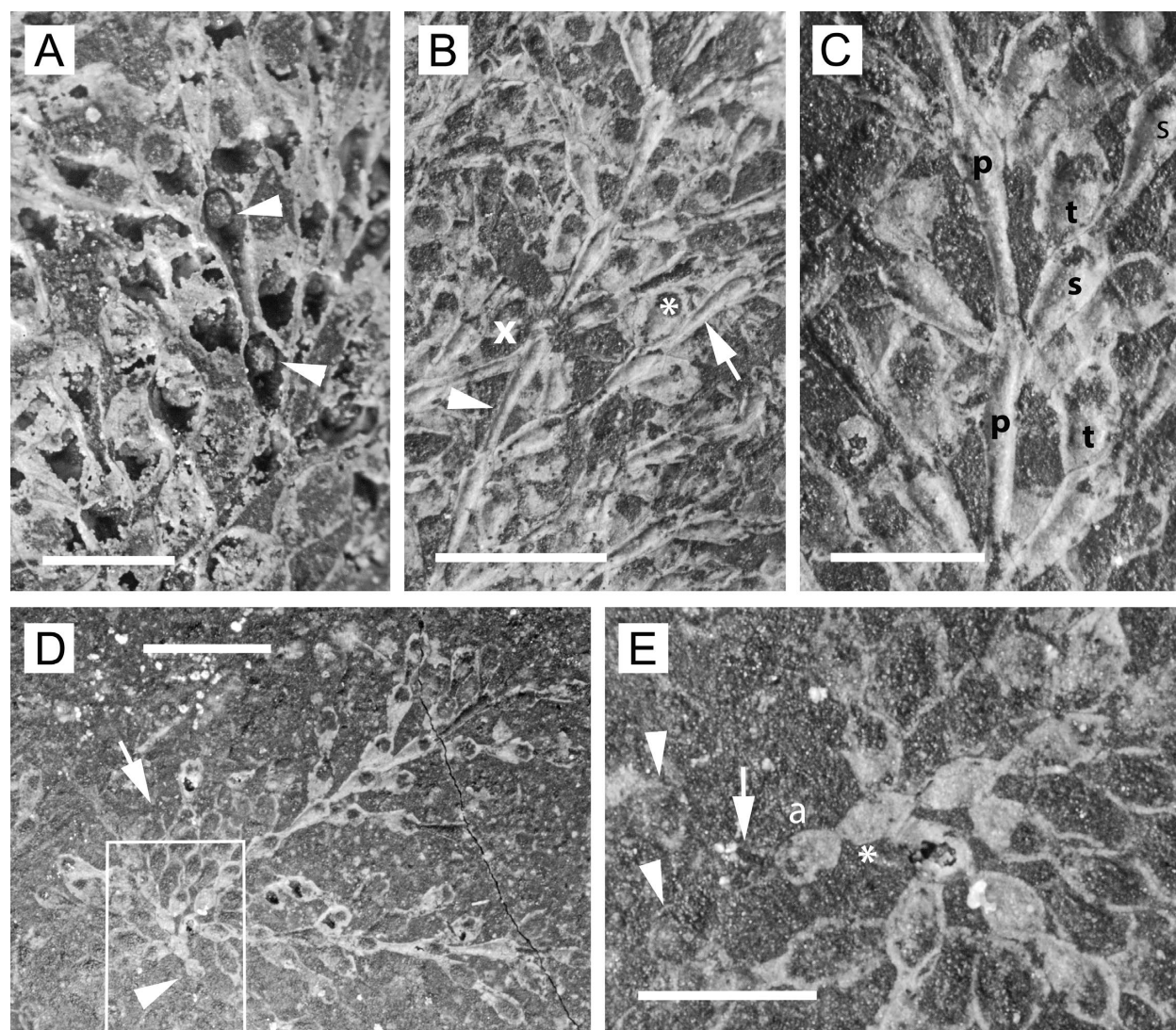


Figure 13. *Incertae sedis* C, photomicrographs of intact specimen NMNS PA18437. **A**, portion of colony in basal view, with rock matrix eroded from interior of some zooids; arrowheads, outline of opesia evident in zooidal interior. **B**, portion of colony in basal view: arrowhead, primary axial zooid; arrow, secondary axial zooid; asterisk, tertiary zooid; x, primary or secondary axis of one branch overlapping primary axis of another branch. **C**, portion of branch in basal view, showing zooids in primary (p) and secondary (s) axes, and tertiary zooids (t). **D**, young colony in basal view, arising from presumed ancestrula (arrowhead). Box indicates region enlarged in panel E. Arrow indicates pluriserial portion of colony. **E**, presumed ancestrula (a) and zone of astogenetic change, seen in basal view, enlarged from boxed area in panel D but rotated clockwise 90 degrees: asterisk, zooid which might alternatively be ancestrula; arrow, zooid budded distolaterally from presumed ancestrula “a”; arrowheads, zooids budded from zooid marked with arrow. Scale bars: 0.50 mm (A, C, E); 1.0 mm (B, D).

12D, E; 13C), with cauda of variable length; non-calcified portion of basal wall sometimes present. Tertiary zooids relatively short and wide (Figures 12D, E; 13B, C), oval or spindle shaped, often lacking cauda altogether, with relatively large, oval or circular, non-calcified zone in distal part of basal wall. Frontal wall (inferred from two zooids in Figure 13A) transversely highly convex; opesia oval, longer than broad, occupying roughly half the non-caudate portion of frontal wall, apparently oriented nearly

parallel to basal surface of colony. Lateral walls with pair of basal tubular, intramural pore chambers distolaterally, one to three smaller tubular chambers on each side more proximally (Figure 12D, arrowheads), and simple pore distally (Figure 12D, asterisked arrowhead). Zooids in some parts of colony may form pluriserial patches in which zooids interconnect via all pore chambers, as seen in young colony (Figure 13D, E). Basal walls of some primary and secondary axial zooids convex in transverse

section (evident in Figures 12E; 13B, C). Ancestrula (Figure 13D, E) oval, budding one daughter zooid distolaterally and one proximally. Frontal zooidal morphology not directly observed. No evidence of ovicells or avicularia.

Remarks.—Although we initially interpreted this as possibly a branched, erect species, with some branches preserved in such a way that the frontal surfaces of zooids were visible, this is not the case. Flexible, non-calcified joints between zooids (as would be expected in a branched, erect species) are lacking, and what appeared to be opesiae proved to be non-calcified zones in the basal walls, as evidenced by parts of the colony (Figure 13A) in which the matrix has been lost from the interior of zooids. Finally, the colonies in our specimen are essentially two-dimensional; no branches were preserved as tangential cross sections, as might be expected in the preservation of a three-dimensional colony. We interpret cases where zooids or branches overlap one another (Figures 12D, E; 13B) to represent intra-colony overgrowth. A puzzling aspect of preservation is that some primary and secondary axial zooids are not flat on the basal surface, but rather are convex in transverse section (e.g. Figures 12E; 13B, C), as might be expected in the preservation of weakly calcified, cylindrical, erect branches. However, some zooids with a convex cauda have lost the matrix inside the expanded portion of the zooid, confirming that the convex surface is the basal surface.

We saw no indications of ovicells, which should be evident even in basal view if present, and so we consider this species to be of malacostegan rather than neocheilostome grade. In growth form, it resembles the electrid species *Spinicharixa dimorpha* Taylor, 1986a in which long, narrow, caudate axial autozooids bud the next axial zooid distally and paired, non-caudate zooids distolaterally. The resulting colony is pluriserial, with zooids in large parts of the colony packed closely together. In *Incertae sedis* C, primary axial zooids are similarly long and narrow, but give rise distolaterally to similarly narrow secondary axial zooids, which in turn give rise distolaterally to non-caudate zooids that produce further non-caudate zooids distally. The resulting colony is more a jumble of closely packed uniserial branches than a pluriserial sheet. The autozooids in *S. dimorpha* are frontally quite different than those in *Incertae sedis* C. In *S. dimorpha*, the opesia in both axial and non-caudate zooids occupies the entire frontal surface and the gymnocyst is negligible (Taylor, 1986a: fig. 25A), whereas in *Incertae sedis* C, the inferred opesia is oval in outline and occupies one-third or less of the total zooid length. In *S. dimorpha*, the opesia is surrounded by a narrow, granulated cryptocyst and the mural rim bears up to eight pairs of spine bases.

Other genera having uniserial budding and reported from the Cretaceous include *Rhammatopora* Lang, 1915;

Herpetopora Lang, 1914; *Pyripora* d'Orbigny, 1849; and *Pyriporopsis* Pohowsky, 1973. As in axial zooids in *Incertae sedis* C, zooids in *Rhammatopora* have a long cauda and the opesia is similar in size and shape to that inferred for *Incertae sedis* C. In *Rhammatopora* the caudae are much longer and narrower relative to the expanded portion, lateral zooids are budded in a cruciate pattern, and the opesial rim bears the bases of many small spines.

Zooids in *Herpetopora* species (Taylor, 1988b) also have a narrower and often longer cauda relative to the expanded portion than in *Incertae sedis* C. Lateral budding sites in *Herpetopora* involve straight, tubular intramural pores, usually one but sometimes more than one on each side. In contrast, the distolateral pores in *Incertae sedis* C are intramural but are expanded within the wall, and zooids often have an additional two lateral intramural pores more proximally on each side, although no budding was observed from these lateral pores. Zooids in some *Herpetopora* species have a relatively small, oval opesia as in *Incertae sedis* C, with the cryptocyst narrow and non-granulated.

The distinctions between *Pyripora* and *Pyriporopsis* are not entirely clear; Taylor (1994) noted that *Pyripora* species have a better developed proximal gymnocyst (presumably, longer cauda and/or smaller opesia; see also Thomas and Larwood, 1960) than *Pyriporopsis*; the cryptocyst is narrow and granulose (pustulose), whereas that in *Pyriporopsis* is striated or lacking. Taylor (1987) noted the following features characteristic of *Pyriporopsis* but did not contrast these with the character states in *Pyripora*: zooids predominantly oval in crowded areas of colony, but pyriform (with caudae) in uniserial series in less crowded areas; spines lacking; calcified closure plates occur; the pore chambers are dilated intramural cavities; and the ancestrula is small, oval, budding daughter zooids distally and proximally (the pattern is different in *Pyripora catenularia*; Taylor, 1986b).

Available evidence suggests placement in *Pyriporopsis*. Our specimen is similar to *Pyriporopsis portlandensis*, the type species of *Pyriporopsis*, in the branching pattern and distribution of caudate and non-caudate zooids (Pohowsky, 1973: fig. 1), and in having intramural pore chambers distolaterally, with one or two pores present more proximally on each side. While we infer the opesia to be smaller in our specimen than in *P. portlandensis*, this was based on only two axial zooids, and tertiary zooids could in fact have a larger opesia. Finally, the early budding pattern (Figure 13D, E) in our specimen seems more similar to that in *P. portlandensis* than in *Pyripora catenularia*, although which zooid in our specimen is the ancestrula is somewhat ambiguous. We interpret zooid "a" in Figure 13E to be the ancestrula, giving rise to one daughter zooid (arrow) distolaterally and another (aster-

isk) proximally. We infer the polarity of the ancestrula from the dark, non-calcified basal area, which is presumably distal as in other zooids. The distolaterally budded daughter zooid in turn appears to give rise to a distal zooid and one distolateral zooid, though these zooids are not well preserved. The zooid proximally budded from the ancestrula buds a triplet of zooids distally and distolaterally, each of which in turn buds distally, as well as distolaterally on one or both sides. *Pyriporopsis portlandensis* shows a similar pattern (Taylor, 1986b: fig. 6) in that the ancestrula buds from the distal and proximal ends, but not laterally. We note, however, that correct identification of the ancestrula is crucial; if the asterisked zooid in Fig. 13E is actually the ancestrula, and if the polarity is in the opposite direction (distal to the right), then the budding pattern is more like that in *Pyripora catenularia* than in *Pyriporopsis portlandensis*.

We refrain from assigning our specimen to a genus, even tentatively, because we were unable to observe key frontal features necessary for generic determination. These include variation in the extent of the opesia; the nature of the cryptocyst, if present; and the presence or absence of opesial spine bases, zooidal closure plates, and kenozooids (the narrowness of some the axial zooids raises the possibility that they are kenozooids).

Suborder Flustrina Smitt, 1868
 Superfamily Calloporoidea Norman, 1903
 Family Calloporidae Norman, 1903
 Genus *Marginaria* Römer, 1840

Type species.—*Cellepora elliptica* von Hagenow, 1839.

Marginaria prolixa sp. nov.

Figures 14, 15

Diagnosis.—Colony encrusting, unilaminar, sheet-like. Zooids in zone of astogenetic change oval or hexagonal; those in zone of repetition elongate, and rectangular or nearly so; opesia oval or elongate. Zooids closely set; proximal gymnocyst up to one-quarter length of some zooids, lateral gymnocyst negligible. Cryptocyst coarsely granulose. Interzooidal avicularia common proximodistally or laterally between zooids. Ooecium globose, prominent, lying on gymnocyst of next-distal zooid; subimmersed in older zooids. Ancestrula budding triplet of daughter zooids distally; subsequent periancestrular zooids include large proximolateral pair, with smaller presumed kenozooid between them. Single or paired distal and one or two pairs of distolateral buttressed recesses leading to multiporous septula. Mural spines and closure plates lacking.

Etymology.— The specific name is an adjective from

the Latin *prolixus* (long, drawn out), referring to the elongate zooids.

Material examined.—Seven specimens from Locs. 3 and 4. Holotype: NMNS PA18438 (Loc. 3). Paratypes: NMNS PA18439–18441 (Loc. 3). See Table 1.

Measurements.—See Table 3.

Description.—Colony (Figure 14A, B) encrusting, unilaminar, sheet-like. Zooids arranged in quincunx (Figure 14E, F) or somewhat irregularly (upper right, Figure 14D); zooids small and irregularly hexagonal or oval in zone of astogenetic change (Figures 14A; 15B, D), but longer in zone of astogenetic change (Figure 14D–F); also compare ZL measurements between NMNS PA18440 and NMNS PA18438 (Table 3). Ovicelled zooids long-oval or rectangular (Figure 14E, F), delineated laterally by narrow groove. Opesia occupying most of zooid length in young zooids, roughly two-thirds in ovicelled zooids. Opesial rim raised, rounded, coarsely and densely granulose; sloping cryptocyst lacking, except as interior side of opesial rim. Mural spine bases not observed. Interzooidal avicularia common, forming at zooidal margin (Figure 15B) distal or distolateral to autozooids; abundant in interzooidal grooves in zone of astogenetic repetition (Figures 14C, D; 15A); sometimes less abundant in zone of astogenetic change (Figures 14A, B; 15D); longer than broad, with short, smooth gymnocystal area proximally and coarsely granulose rostrum (Figure 15C); no hinge structures observed. Some avicularia have elongate opesial opening, truncate at one end, tapering toward other, with narrow end directed proximally (e.g. Figure 14F); others have irregular, circular, or oval opening. Among ovicelled zooids, avicularia often lateral to ovicell (Figure 14E, F). Ovicell (Figure 14E, F) slightly wider than long, nearly as wide as autozooids, lying on proximal gymnocyst of zooid distal to maternal zooid; initially prominent (Figure 14E) but partly immersed with increased calcification (Figure 14F). Form of interzooidal connections ambiguous due to poor preservation or casting limitations; zooids have pair of small, distal buttressed recesses (arrowheads, Figure 14D) and one or two pairs of distolateral buttressed recesses (Figures 14D, 15A) that appear to lead to multiporous septula; autozooids interconnect with interzooidal avicularia as well as neighboring autozooids. Ancestrula (Figure 15B, D) oval or rectangular, surrounded by a triplet of daughter zooids distally, a presumed kenozooidal chamber proximally, and a pair of larger periancestrular zooids proximolaterally.

Remarks.—Most of the approximately 15 known species of *Marginaria* (Bock, 2017) were described from the Late Cretaceous, although two have been reported from the Paleogene (Berthelsen, 1962; Guha and Gopikrishna, 2007). Species in *Marginaria* characteristically have numerous small interzooidal avicularia scattered among

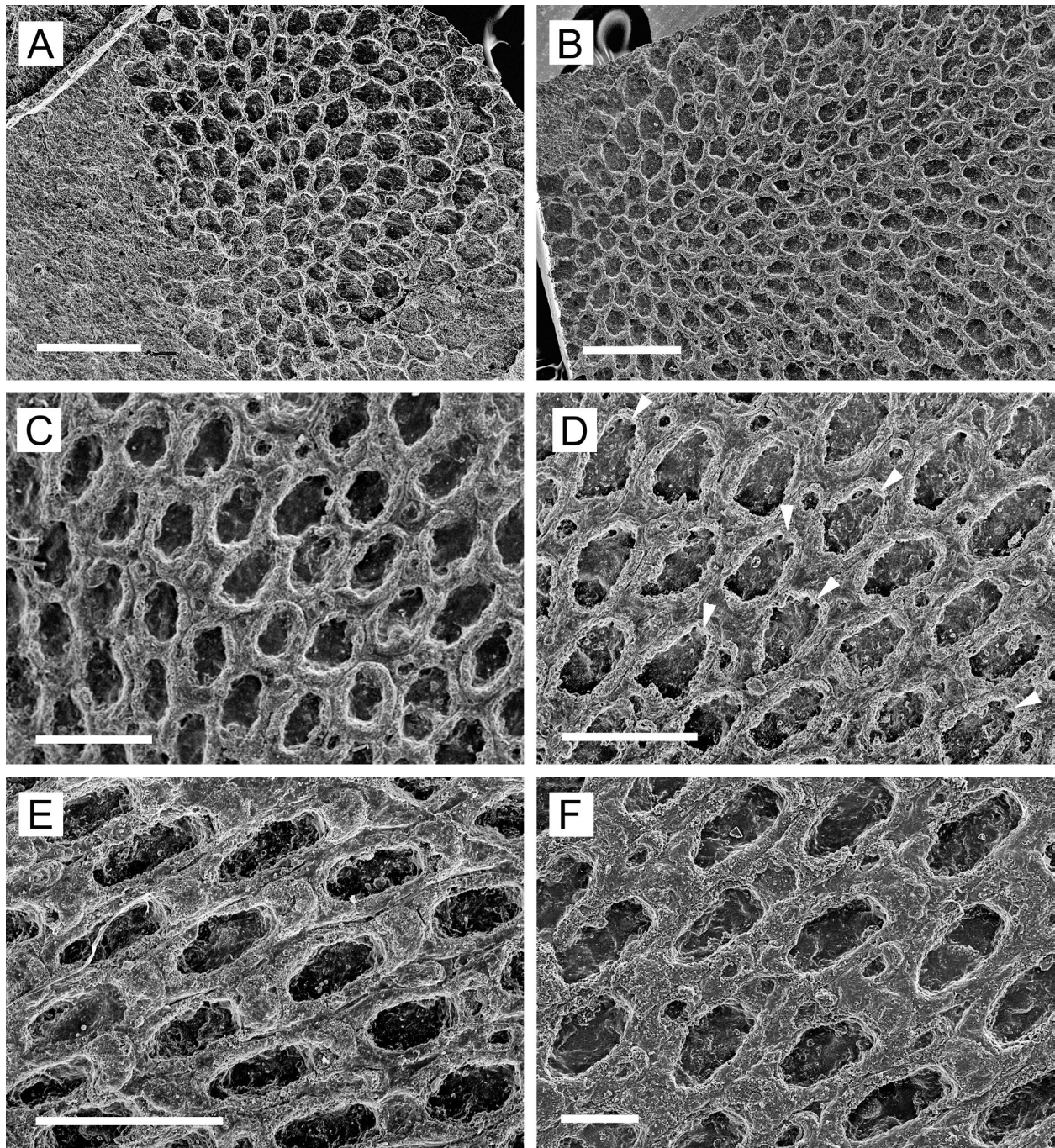


Figure 14. *Marginaria proluxa* sp. nov., SEM images of silicone casts from colony molds. **A**, paratype NMNS PA18439, young colony; **B**, paratype NMNS PA18441, colony, showing oval autozooids in zone of astogenetic change (left) and more-elongate autozooids in zone of astogenetic repetition (right); **C**, NMNS PA18440, mixed oval and elongate autozooids, with scattered interzooidal avicularia; **D–F**, holotype, NMNS PA18438; **D**, autozooids and interzooidal avicularia; arrowheads, distal buttressed recesses; **E**, ovicelled zooids; **F**, ovicelled zooids in older, more heavily calcified portion of colony, showing partly immersed oecia and interzooidal avicularia. Scale bars: 1.0 mm (A, B); 0.50 mm (C–E); 0.20 mm (F).

autozooids; these avicularia are budded at the colony margin, along with developing autozooids (Taylor and McKinney, 2006), and commonly lack calcified hinge-

support structures, leading some authors (e.g. Guha and Gopikrishna, 2007) to refer to them as kenozooids rather than avicularia. However, they are distributed as one

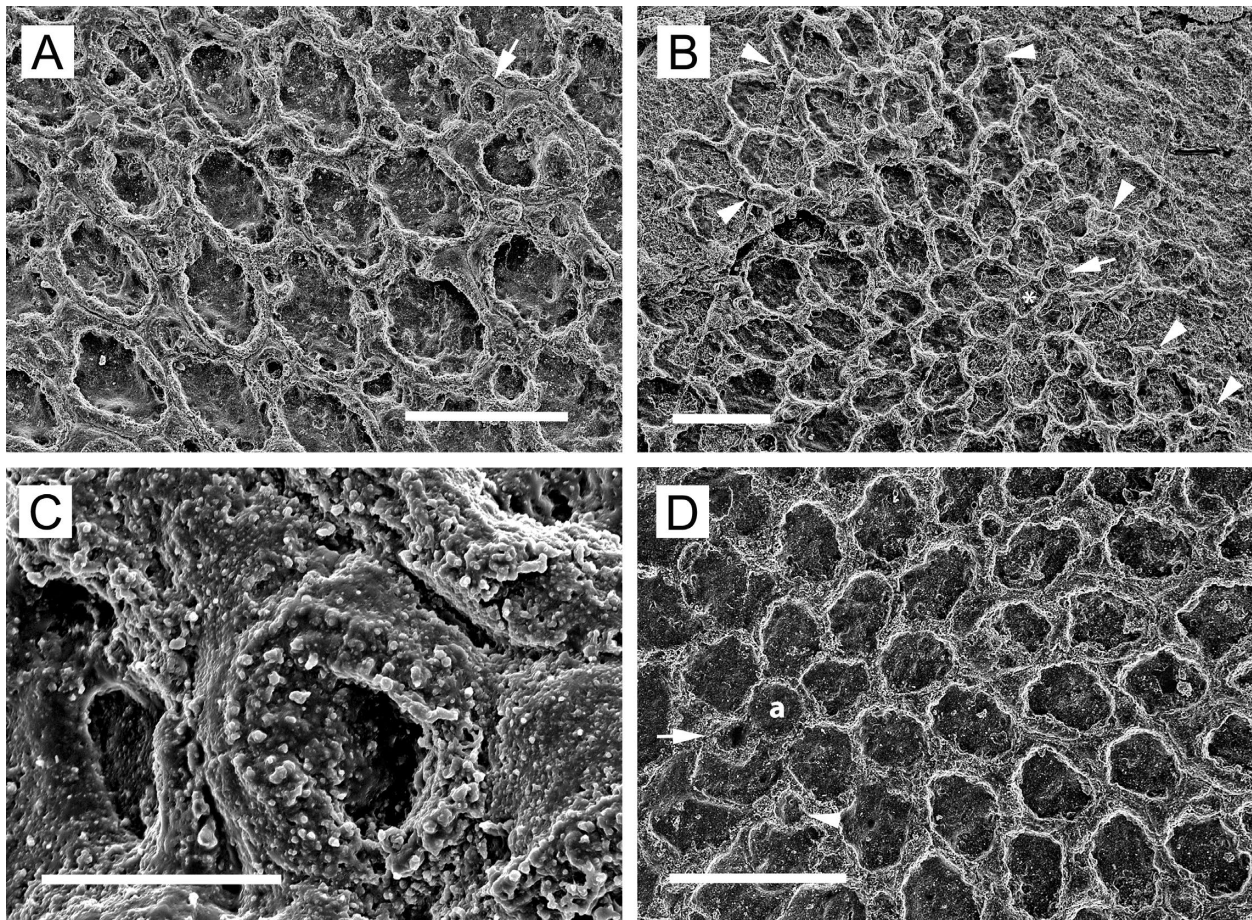


Figure 15. *Marginaria prolixa* sp. nov., SEM images of silicone casts from colony molds; A, C, D, paratype NMNS PA18441; B, paratype NMNS PA18439; A, autozooids, showing interzooidal connections; distal direction toward lower right; arrow, interzooidal avicularium enlarged in panel C; B, paratype NMNS PA18441, young colony, with arrowheads indicating avicularia forming at or near colony margin; asterisk, presumed ancestrula; arrow, presumed kenozooidal chamber budded proximally from ancestrula; C, enlargement of interzooidal avicularium indicated by arrow in panel A; D, ancestrula (a) and periancestrular zooids enlarged from colony in Figure 14B; arrow, presumed kenozooidal chamber budded proximally from ancestrula, lying between paired proximolateral zooids; arrowhead, another kenozooidal chamber early in astogeny. Scale bars: 0.50 mm (A, B, D); 0.10 mm (C).

would expect for avicularia. These putative avicularia appear to lack skeletal hinge support structures in various species of *Marginaria*, but whatever their function, they constitute a shared character for the genus.

The genus *Reptoflustrella* d'Orbigny, 1853 is similar to *Marginaria* but supposedly differs from the latter in having the interzooidal avicularia in a stereotyped position proximolateral to most autozooids; in addition, the generic description of *Reptoflustrella* includes zooids having at least two pairs of distal spine bases and the proximal gymnocyst comprising a quarter to two-thirds the zooidal length (Gordon and Taylor, 2005). The distinctions between the genera are somewhat unclear, as some of the avicularia in *R. cenomana* d'Orbigny, 1853, the type species of *Reptoflustrella*, are arguably not in the proximo-

lateral position (Gordon and Taylor, 2005: fig. 1D), and some species in *Marginaria* have spines and an extensive proximal gymnocyst, as in *Reptoflustrella*. Voigt (1989) included *R. cenomana* in *Marginaria* in a review of the latter genus, thus reducing *Reptoflustrella* to a junior synonym of *Marginaria*. In our holotype specimen of *M. prolixa*, the interzooidal avicularia are commonly in the proximolateral position in the vicinity of ovicelled zooids (Figure 14E, F), but in non-reproducing parts of the colony, they are often positioned proximodistally between successive autozooids (Figure 14D). Furthermore, zooids in *M. prolixa* lack spines, as is the case in about half the species in *Marginaria*. While Gordon and Taylor (2005) believed that it was premature to include *Reptoflustrella* in *Marginaria*, our species appears in any case to fit better

Table 3. Measurements (in millimeters) for *Marginaria prolixa* sp. nov. For each set of values, the top row is the range and the bottom row the mean and standard deviation.

	Holotype	Paratype
	NMNS PA18438	NMNS PA18440
Autozooid length	0.41–0.63 0.510±0.054	0.33–0.46 0.418±0.035
Autozooid width	0.22–0.31 0.273±0.028	0.23–0.32 0.265±0.024
Autozooid opesia length	0.23–0.41 0.326±0.050	0.24–0.34 0.288±0.032
Autozooid opesia width	0.15–0.19 0.170±0.010	0.14–0.20 0.167±0.031
Ovicell length	0.11–0.15 0.134±0.007	–
Ovicell width	0.15–0.18 0.161±0.010	–
Avicularium length	0.13–0.21 0.153±0.019	0.13–0.20 0.167±0.016
Avicularium width	0.09–0.13 0.099±0.011	0.08–0.12 0.099±0.010
Sample size (<i>n</i>)	15	15

Table 4. Cheilostome bryozoan species detected in the Upper Cretaceous Himenoura Group, Shimokoshikijima Island, Japan, with the number of specimens from each locality.

Species	Locality			
	1	2	3	4
<i>Kenocharixa kashimaensis</i>	7	–	27	1
<i>Charixa</i> sp. A	1	–	–	–
<i>Incertae sedis</i> A	–	–	1	–
<i>Incertae sedis</i> B	1	–	–	–
<i>Incertae sedis</i> C	–	1	–	–
<i>Marginaria prolixa</i>	–	–	6	1

in *Marginaria*.

Most species in *Marginaria* have zooids less than 0.40 mm long, typically with an oval or elliptical opesia, and with gymnocyst evident both proximally and laterally. Another species with larger zooids is *M. caminoides* (Voigt, 1967) ($ZL \times ZW = 0.60 \times 0.45$ mm), which, although encrusting, differs from *M. prolixa* in forming

narrowly pluriserial branches; zooids are short-oval or hexagonal in outline; the opesia is oval to elliptical; the interzooidal avicularia are large; and zooids have mural spines.

Discussion

We detected six cheilostome species but no cyclostomes. Among the cheilostomes, five (83%) were of malacostegan-anascan grade, and one (*Marginaria prolixa*) was a neocheilostome anascan. *Kenocharixa kashimaensis* was the commonest species overall, occurring at three of the four sites and abundant at Loc. 3 (Table 4). *Marginaria prolixa* was moderately abundant at Loc. 3 and also occurred at Loc. 4. The other four species were detected as one colony each, and were not well enough preserved to identify to species (*Charixa* sp. A) or genus (*Incertae sedis* A, B, C). Locs. 1 and 3 showed equivalent diversity, with three species each, with the other localities having one or two species.

In a tabulation of Late Cretaceous (Campanian–Maasrichtian) regional diversity in the southeastern USA, Taylor and McKinney (2006) reported 130 bryozoan species representing 77 genera, including 34 (26%) cyclostomes, 11 (8%) malacostegan cheilostomes, 44 (34%) anascan-grade neocheilostomes, 27 (21%) cribrimorph-grade neocheilostomes, and 14 (11%) ascophoran-grade neocheilostomes, noting that extensive collections remain to be studied and will certainly add to the known diversity. In the southeastern USA, then, cyclostomes comprise about one-quarter of the total diversity, and among 96 cheilostomes, species of the more primitive (*sensu* Taylor, 1988a) malacostegan grade occupy only 11%, with neocheilostomes comprising 89%. Though Taylor and McKinney (2006) did not report local diversities, McKinney and Taylor (2016) tabulated a diversity of six cyclostome (26%) and 17 cheilostome (74%) species from the Ripley Formation (Maastrichtian) at Coon Creek, Tennessee, within the area of the Taylor and McKinney (2006) study; among the 17 cheilostomes were four malacostegans (23%) and 13 (77%) neocheilostomes, including seven anascans (41%), three cribrimorphs (18%), and three ascophorans (18%). The local sample roughly mirrored the regional sample, with about one-quarter cyclostomes and a low proportion of malacostegans compared to neocheilostomes.

Compared to the Campanian–Maastrichtian fauna in the southeastern USA, the lower to middle Campanian fauna detected on Shimokoshikijima was depauperate, in both species diversity (six species) and morphological range, or disparity (no cyclostomes; five (83%) malacostegan cheilostomes; one anascan-grade (17%) neocheilostome; no cribrimorphs or ascophorans). The differences in diversity

between our sample and the regional and local samples from the southeastern USA mentioned above seem too extreme to be attributed to the low sample size in our study. Other surveys of nearshore, bivalve-encrusting Cretaceous faunas in Japan have been similarly depauperate: one malacostegan species of early to middle Cenomanian age from the Yezo Group in northern Japan (Ostrovsky *et al.*, 2006), and four malacostegan and two anascan-grade neocheilostome species of Albian to early Cenomanian age from the Goshoura Group, Kyushu, Japan. In these studies, as in ours, the bryozoans were rather poorly preserved, occurring primarily as basal colony surfaces or colony molds detached from the substrate; only rarely have specimens been found with the calcified frontal surface exposed.

From their analyses of carbonate platform biota along the NW Pacific margin, Iba and Sano (2007) concluded that the biota in this region belonged to the Tethyan biotic realm in the interval from the Middle Jurassic to early Albian, but became isolated from the latter between the latest Aptian and middle Albian as the NW Pacific became separate from the Tethyan realm. Molluscan genera subsequently began to evolve new species, leading to establishment of the North Pacific biotic province. We offer the hypothesis that the low-diversity, low-disparity bryozoan assemblages in Japan detected in the upper Albian–lower Cenomanian Goshoura Group (Dick *et al.*, 2013) and in the lower to middle Campanian Himenoura Group (this study) may represent a relict fauna—that is, the descendants of lineages present in the North Pacific at the time this region became isolated from the Tethys. Within these relict lineages, relatively little innovation occurred, in contrast to the western Tethys, where morphological innovation led to diverse faunas that included cribrimorphs and ascophorans. This would explain the failure to date to detect cribrimorph or ascophoran cheilostomes in Cretaceous deposits in Japan.

The fossil record lends some support to this hypothesis. The oldest cheilostome ovicells are known in the genera *Wilbertopora* and *Marginaria* from the late Albian (Ostrovsky and Taylor, 2004), and hence *Marginaria*, which we detected on Shimokoshikijima, could have been among the lineages retained in the NW Pacific after isolation from the Tethys, assuming a slightly earlier origin of ovicells than has been detected to date. Similarly, *Charixa* is known from the Hauterivian to late Albian (Early Cretaceous) (Ostrovsky *et al.*, 2008) in the western Tethys, and could have been among the lineages retained in the NW Pacific. Finally, the earliest records available for species in the malacostegan family Chiplonkarinidae, to which we tentatively attribute *Incertae sedis* B, are for *Chiplonkarina bretoni* Taylor and Badve, 1995, from the early Cenomanian of France and Germany. However,

publication is pending for a new genus and species of late Albian age in this family (Paul Taylor, personal communication), which again does not greatly postdate a presumed early to middle Albian separation of the regions. In contrast, the earliest cribrimorphs did not appear until the early Cenomanian (Larwood, 1985), and the earliest species inferred to have an ascus appeared in the Coniacian (Gordon, 2000). The origins of these novelties in Western-Tethys species thus clearly postdated the presumed isolation of malacostegan and anascan-grade neocheilostome lineages in the NW Pacific in the latest Aptian to middle Albian interval.

The isolation hypothesis to explain low Late Cretaceous cheilostome diversity and disparity in the NW Pacific can be tested with further sampling. Discovery of a Late Cretaceous bryozoan assemblage in eastern Asia containing cribrimorphs and ascophorans, for example, would negate the hypothesis, to the extent that the high-diversity deposit did not reflect the reestablishment of exchange between the NW Pacific and the Tethys. Exchange was reestablished at some point, although when this occurred is not clear; Iba and Sano (2007) noted that the carbonate platform biota became reestablished in the NW Pacific in the Eocene, which would imply reconnection with the Tethys. If further sampling continues to find low Late Cretaceous cheilostome diversity and disparity in the NW Pacific, with a dramatic increase in the Early Paleogene, this would support the isolation hypothesis.

Acknowledgments

We thank Yuka Miyake (Kumamoto University) for assistance in the field; the Kashima Town government for logistical support; and Dennis Gordon and Paul Taylor for substantial peer reviews. This study was funded in part by a Grant-in-Aid for Scientific Research (KAKENHI) to T. Komatsu (16K05593) from the Japan Society for the Promotion of Science.

References

- Allman, G. J., 1856: *A Monograph of the Freshwater Polyzoa, Including All the Known Species, both British and Foreign*, vii + 119 p., 11 pls. Ray Society, London.
- Aramaki, M., Komatsu, T., Miyake, Y., Takahashi, O. and Tsutsumi, Y., 2013: Radiolarians from the Upper Cretaceous Himenoura Group, Nakakoshiki-jima Island, Kagoshima Prefecture, Japan. *Journal of the Geological Society of Japan*, vol. 119, p. 45–50. (in Japanese with English abstract)
- Berthelsen, O., 1962: Cheilostome Bryozoa in the Danian deposits of east Denmark. *Danmarks Geologiske Undersøgelse*, vol. 83, p. 1–290.
- Bock, P., 2017: *Indexes to Bryozoan Taxa* [online]. [Cited June 2017]. Available from: <http://www.bryozoa.net/indexes.html>.
- Busk, G., 1852a: An account of the Polyzoa, and sertularian zoo-

- phytes, collected in the voyage of the *Rattlesnake*, on the coasts of Australia and the Louisiade Archipelago. In, MacGillivray, J. ed., *Narrative of the Voyage of H. M. S. Rattlesnake, Volume 1*, p. 343–402, pl. 1 (Appendix No. IV). T. W. Boone, London.
- Busk, G., 1852b: *Catalogue of Marine Polyzoa in the Collection of the British Museum. I. Cheilostomata*, 54 p. Trustees of the British Museum, London.
- Dalrymple, R. W., 1992: Tidal depositional systems. In, Walker, R. G. and James, N. P. eds., *Facies Models-Response to Sea-Level Changes*, p. 195–218. Geological Association of Canada, St. John's.
- Dick, M. H., Komatsu, T., Takashima, R. and Ostrovsky, A. N., 2013: A mid-Cretaceous (Albian–Cenomanian) shell-rubble bryozoan fauna from the Goshoura Group, Kyushu, Japan. *Journal of Systematic Palaeontology*, vol. 12, p. 401–425.
- Dick, M. H., Osawa, T. and Nodasaka, Y., 2009: Method for making detailed, SEM-suitable VPS silicone casts of colony molds from fossil bryozoans. *Paleontological Research*, vol. 13, p. 193–197.
- Gordon, D. P., 2000: Towards a phylogeny of cheilostomes—morphological models of frontal wall/shield evolution. In, Herrera-Cubilla, A. and Jackson, J. B. C. eds., *Proceedings of the 11th International Bryozoology Association Conference*, p. 17–37. Smithsonian Tropical Research Institute, Balboa.
- Gordon, D. P., 2017: *Bryozoa: Cheilostomata. Interim Classification for Treatise, Version of 8 September 2017*. 16 p. Institute of Water and Atmospheric Research, Wellington. (*Unpublished but widely circulated document obtained from the author*)
- Gordon, D. P. and Taylor, P. D., 2005: The cheilostomatous genera of Alcide d'Orbigny—nomenclatural and taxonomic status. In, Hayward, H. I., Cancino, J. M. and Wyse Jackson, P. I. eds., *Bryozoan Studies 2004*, p. 83–97. Taylor and Francis, London.
- Gordon, D. P. and Taylor, P. D., 2015: Bryozoa of the Early Eocene Tumaio Limestone, Chatham Island, New Zealand. *Journal of Systematic Palaeontology*, vol. 13, p. 983–1070.
- Gray, J. E., 1848: *List of the Specimens of British Animals in the Collection of the British Museum. Part 1. Centroniae or Radiated Animals*, p. xiii + 173. Trustees of the British Museum, London.
- Guha, A. K. and Gopikrishna, K., 2007: New calloporid (Bryozoa, Cheilostomata) species from Tertiary sequences of western Kachchh, Gujarat. *Journal of the Geological Society of India*, vol. 70, p. 121–130.
- Hagenow, F. von, 1839: Monographie der Rügen'schen Kreide-Versteinerungen. Abt. 1. Phytolithen und Polyparien. *Neues Jahrbuch für Geognosie, Geologie und Petrefaktenkunde*, Band 1839, p. 252–296.
- Iba, Y. and Sano, S., 2007: Mid-Cretaceous step-wise demise of the carbonate platform biota in the Northwest Pacific and establishment of the North Pacific biotic province. *Palaeogeography, Palaeoclimatology, Palaeoecology*, vol. 245, p. 462–482.
- Iba, T. and Sano, S., 2008: Paleobiogeography of the pectinid bivalve *Neithea*, and its pattern of step-wise demise in the Albian Northwest Pacific. *Palaeogeography, Palaeoclimatology, Palaeoecology*, vol. 267, p. 138–146.
- Inoue, E., Tanaka, K. and Teraoka, Y., 1982: *Geology of the Nakakoshiki District with Geological Sheet Map at 1:50,000*, 99 p. Geological Survey of Japan, Tsukuba. (*in Japanese with English abstract*)
- Kanoh, M., Toshimitsu, S. and Tashiro, M., 1989: Stratigraphy and depositional facies of the Himenoura Group in the Koshikijima Island, Kagoshima Prefecture. *Research Reports of the Kochi University, Natural Science*, vol. 38, p. 157–172. (*in Japanese with English abstract*)
- Kojo, Y., Komatsu, T., Iwamoto, T., Takashima, R., Takahashi, O. and Nishi, H., 2011: Stratigraphy and detailed age of the Upper Cretaceous Himenoura Group in the eastern part of Amakusa-Kamishima Island, Kumamoto, Japan. *Journal of the Geological Society of Japan*, vol. 117, p. 398–416. (*in Japanese with English abstract*)
- Komatsu, T. and Maeda, H., 2005: Stratigraphy and fossil bivalve assemblages of the mid-Cretaceous Goshoura Group, southwest Japan. *Paleontological Research*, vol. 9, p. 119–142.
- Komatsu, T., Miyake, Y., Manabe, M., Hirayama, R., Yabumoto, Y. and Tsuihiji, T., 2014: Stratigraphy, fossils and depositional environments of the Upper Cretaceous Himenoura Group on the Koshikijima Islands. *Journal of the Geological Society of Japan*, vol. 120, Supplement, p. 19–39. (*in Japanese with English title*)
- Komatsu T., Ono M., Naruse, H. and Kumagae, T., 2008: Upper Cretaceous depositional environments and bivalve assemblages of far-east Asia: the Himenoura Group, Kyushu, Japan. *Cretaceous Research*, vol. 29, p. 489–508.
- Lang, W. D., 1914: On *Herpetopora*, a new genus containing three new species of Cretaceous cheilostome Polyzoa. *Geological Magazine*, vol. 51, p. 5–8.
- Lang, W. D., 1915: On some new uniserial Cretaceous cheilostome Polyzoa. *Geological Magazine, new series, decade 6*, vol. 2, p. 496–504.
- Larwood, G. P., 1985: Form and evolution of Cretaceous myagromorph Bryozoa. In, Nielsen, C. and Larwood, G. P. eds., *Bryozoa: Ordovician to Recent*, p. 169–174. Olsen and Olsen, Fredensborg.
- Levensen, G. M. R., 1902: Studies on Bryozoa. *Videnskabelige Meddelelser fra den Naturhistoriske Forening i Kjobenhavn*, vol. 54, p. 1–31.
- Linnaeus, C., 1767: *Systema Naturae. Tomus 1, Regnum Animale. 12th edition*, 1327 p. Laurentii Salvii, Holmiae.
- McKinney, F. K. and Taylor, P. D., 2016: The premier North American Maastrichtian bryozoan fauna: Coon Creek, Tennessee. *Bulletin of the Alabama Museum of Natural History* 33, vol. 2, p. 1–6.
- Misaki, A., Komatsu, T. and Miyake, Y., 2016: A Late Cretaceous ammonoid *Eulophoceras* (Sphenodiscidae) from the Koshikijima Islands, southwestern Kyushu, Japan. *Abstracts with Proceedings, 2016 Annual Meeting of the Palaeontological Society of Japan, Fukui Prefectural University, Fukui*, p. 41. (*in Japanese*)
- Miyake, Y., Aramaki, M., Komatsu, T., Tsuihiji, T., Manabe, M. and Hirayama, R., 2011: Depositional facies containing non-marine vertebrate fossils in the Upper Cretaceous Himenoura Group on the Koshikijima Islands, Kagoshima, Japan. *Journal of the Sedimentological Society of Japan*, vol. 70, 62 p.
- Nishizawa, Y. and Sakagami, S., 1997: Phylogenetic significance of a new cheilostome bryozoan species, *Dysnoetocella ? voigti* from the Upper Cretaceous Izumi Group in Shikoku, Japan. *Paleontological Research*, vol. 1, p. 267–273.
- Noda, M., Ohtsuka, M., Kano, M. and Toshimitsu, S., 1995: The Cretaceous inoceramids from the Mifune and Himenoura Groups in Kyushu. *Geological Society of Oita, Special Issue*, vol. 2, p. 1–63.
- Norman, C. A. M., 1903: Notes on the natural history of East Finmark — Polyzoa. *Annals and Magazine of Natural History, Series 7*, vol. 11, p. 567–598.
- Orbigny, A. D. d', 1849: Description de quelques genres nouveaux de mollusques bryozoaires. *Revue et Magasin de Zoologie, Série 2*, vol. 1, p. 499–504.
- Orbigny, A. D. d', 1853: *Paléontologie Française, Terrains Crétacés, Tome 5, Bryozoaires*, p. 473–984. Victor Masson, Paris.
- Ostrovsky, A. N., Takashima, R., Dick, M. H., Grischenko, A. V., Nishi, H. and Mawatari, S. F., 2006: First record of a Cretaceous cheilostome bryozoan from Hokkaido, Japan. *Cretaceous Research*, vol. 27, p. 859–862.

- Ostrovsky, A. N. and Taylor, P. D., 2004: Systematics of Upper Cretaceous calloporid bryozoans with primitive spinose ovicells. *Palaeontology*, vol. 47, p. 775–793.
- Ostrovsky, A. N., Taylor, P. D., Dick, M. H. and Mawatari, S. F., 2008: Pre-Cenomanian cheilostome Bryozoa: current state of knowledge. In, Okada, H., Mawatari, S. F., Suzuki, N. and Gautam, P. eds., *Origin and Evolution of Natural Diversity*, p. 69–74. Hokkaido University, Sapporo.
- Pohowsky, R. A., 1973: A Jurassic cheilostome from England. In, Larwood, G. P. ed., *Living and Fossil Bryozoa*, p. 447–461. Academic Press, London.
- Römer, F. A., 1840: *Die Versteinerungen des Norddeutschen Kreidegebirges*, 145 p. Han'schen Hofbuchhandlung, Hannover.
- Smitt, F. A., 1868: Bryozoa marina in regionibus arcticis et borealibus viventia recensuit. *Öfversigt af Kongliga Vetenskaps-Akademiens Förhandlingar*, vol. 24, p. 443–4
- Stach, L. W., 1937: Reports of the McCoy Society for Field Investigation and Research. Lady Julia Percy Island. 13. Bryozoa. *Proceedings of the Royal Society of Victoria (New Series)*, vol. 49, p. 373–384.
- Tanaka, K. and Teraoka, T., 1973: Stratigraphy and sedimentation of the Upper Cretaceous Himenoura Group in Koshiki-jima, southwest Kyushu, Japan. *Bulletin of the Geological Survey of Japan*, vol. 24, p. 157–184. (in Japanese with English translation of title and English abstract)
- Tashiro, M., 1976: Bivalve faunas of the Cretaceous Himenoura Group in Kyusyu. *Palaeontological Society of Japan, Special Paper*, vol. 19, p. 1–102.
- Tashiro, M., Taniuchi, Y., Okamura, M., Yasuda, H. and Maeda, H., 1986: Sedimentary environments of the lower part of the Himenoura Group, Amakusa-Kamishima, Kumamoto Prefecture, southwest Japan. *Research Reports of Kochi University*, vol. 35, p. 151–179. (in Japanese with English abstract)
- Taylor, P. D., 1986a: *Charixa* Lang and *Spinicharixa* gen. nov., cheilostome bryozoans from the Lower Cretaceous. *Bulletin of the British Museum (Natural History), Geology Series*, vol. 40, p. 197–222.
- Taylor, P. D., 1986b: The ancestrula and early growth pattern in two primitive cheilostome bryozoans: *Pyripora catenularia* (Fleming) and *Pyriporopsis portlandensis* Pohowsky. *Journal of Natural History*, vol. 20, p. 101–110.
- Taylor, P. D., 1987: Skeletal morphology of malacostegan grade cheilostome Bryozoa. In, Ross, J. R. P. ed., *Bryozoa: Past and Present*, p. 269–276. Western Washington University, Bellingham.
- Taylor, P. D., 1988a: Major radiation of cheilostome bryozoans: triggered by the evolution of a new larval type? *Historical Biology*, vol. 1, p. 45–64.
- Taylor, P. D., 1988b: Colony growth pattern and astogenetic gradients in the Cretaceous cheilostome bryozoan *Herpetopora*. *Palaeontology*, vol. 31, p. 519–549.
- Taylor, P. D., 1994: An early cheilostome bryozoan from the Upper Jurassic of Yemen. *Neues Jahrbuch für Geologie und Paläontologie Abhandlungen*, Band 191, p. 331–344.
- Taylor, P. D., 2008: Late Cretaceous bryozoans from California and Baja California. *Journal of Paleontology*, vol. 82, p. 823–834.
- Taylor, P. D. and Badve, R. M., 1994: The mid-Cretaceous bryozoan fauna from the Bagh Beds of central India: composition and evolutionary significance. In, Hayward, P. J., Ryland, J. S. and Taylor, P. D. eds., *Biology and Palaeobiology of Bryozoans*, p. 181–186. Olsen and Olsen, Fredensborg.
- Taylor, P. D. and Badve, R. M., 1995: A new cheilostome bryozoan from the Cretaceous of India and Europe: a cyclostome homeomorph. *Palaeontology*, vol. 38, p. 627–657.
- Taylor, P. D. and Gordon, D. P., 2007: Bryozoans from the Late Cretaceous Kahuitara Tuff of the Chatham Islands, New Zealand. *Alcheringa*, vol. 31, p. 339–363.
- Taylor, P. D. and McKinney, F. K., 2006: Cretaceous Bryozoa from the Campanian and Maastrichtian of the Atlantic and Gulf coastal plains, United States. *Scripta Geologica*, vol. 132, p. 1–346.
- Thomas, H. D. and Larwood, G. P., 1960: The Cretaceous species of *Pyripora* d'Orbigny and *Rhammatopora* Lang. *Palaeontology*, vol. 3, p. 370–386.
- Toshimitsu, S., Kano, M. and Tashiro, M., 1990: Oyster reefs from the Upper Himenoura subgroup (Upper Cretaceous), Kyushu, Japan. *Fossils (Palaeontological Society of Japan)*, no. 49, p. 1–12. (in Japanese with English abstract)
- Ueda, Y. and Furukawa, N., 1960: On the Himenoura Group of the Amakusa-Kamishima and adjacent islets, Kumamoto Prefecture. *Scientific Reports of the Department of Geology, Kyushu University*, vol. 5, p. 14–35. (in Japanese)
- Voigt, E., 1967: Oberkreide-Bryozoen aus den asiatischen Gebieten der UdSSR. *Mitteilungen aus dem Geologischen Staatsinstitut in Hamburg*, Heft 36, p. 5–95.
- Voigt, E., 1983: Zur Biogeographie der europäischen Oberkreide-Bryozoenfauna. *Zitteliana*, vol. 10, p. 317–347.
- Voigt, E., 1989: Beitrag zur Bryozoen-Fauna des sächsischen Cenomaniums. *Abhandlungen des Staatlichen Museums für Mineralogie und Geologie zu Dresden*, Band 36, p. 8–87.

Author contributions

TK and CS initiated the study. All authors contributed to fieldwork, though CS and TK conducted most of it. CS made all silicone casts, prepared specimens for SEM, took all SEM images, and preliminarily identified specimens. MHD took light microscopic images of one specimen and made most of the measurements presented. MHD was responsible for taxonomy and wrote most of the manuscript; TK wrote the sections on geological setting. TK prepared Figures 1–6 and MHD prepared Figures 7–15.